

A Dynamical Key to the Riemann Hypothesis  
Chris King Emeritus, University of Auckland 11 May 2011  
v1.12 ( <http://arxiv.org/abs/1105.2103> )

**Abstract:** *This note sets out a dynamical basis for the non-trivial zeros of the Riemann zeta function being on the critical line  $x = \frac{1}{2}$ . It does not prove the Riemann Hypothesis (RH), but it does give a dynamical explanation for why the various forms of zeta and the  $L$ -functions do have their non-trivial zeros on the critical line and why other closely related functions do not. It suggests RH is an additional unprovable postulate of the number system, similar to the axiom of choice, associated with the limiting behavior of the primes as  $n \rightarrow \infty$ .*

The Riemann zeta function  $\zeta(z) = \sum_{n=1}^{\infty} n^{-z} = \prod_{p \text{ prime}} (1 - p^{-z})^{-1}$   $\text{Re}(z) > 1$  is defined as either a sum of complex exponentials over integers, or as a product over primes, due to Euler's prime sieving.

The zeta function is a unitary example of a Dirichlet series  $\sum_{n=1}^{\infty} a_n n^{-z}$ , which are similar to power series except that the terms are complex exponentials of integers, rather than being integer powers of a complex variable as with power series. We shall examine a variety of Dirichlet series to discover which, like zeta, have their non-real zeros on the critical line  $x = \frac{1}{2}$  and which don't.

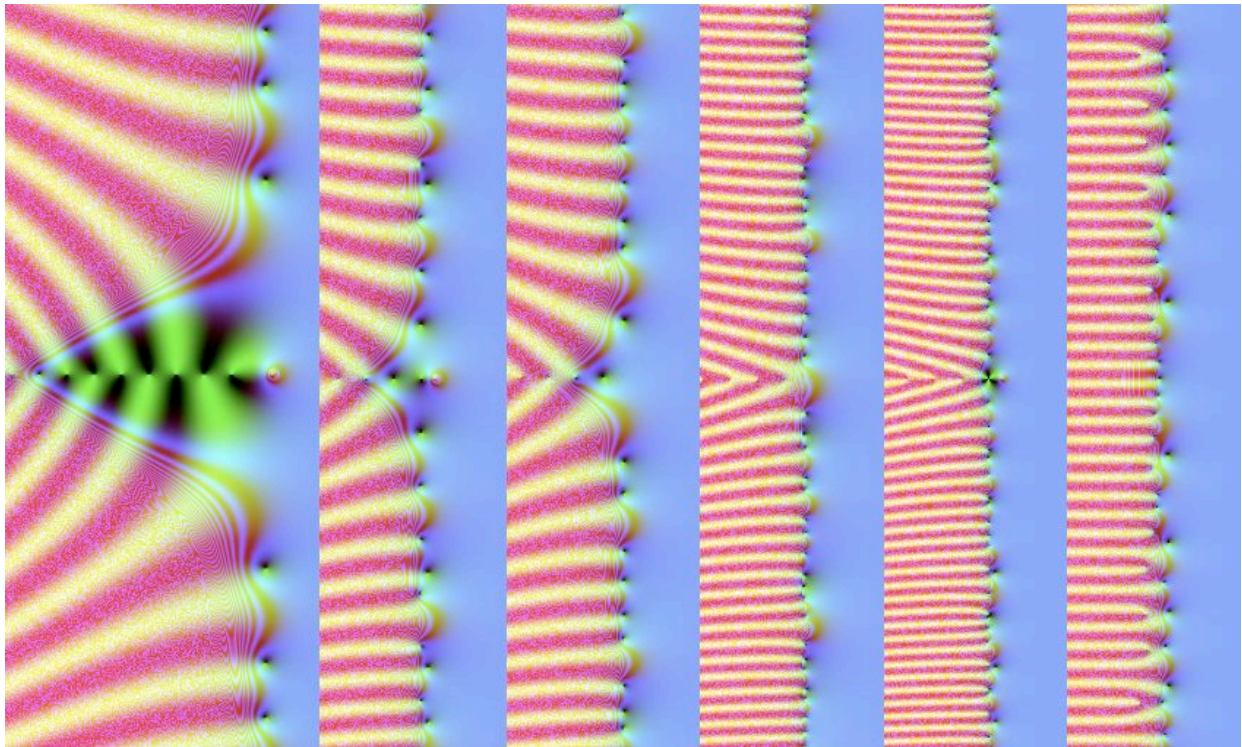


Fig 1: Riemann zeta and Dirichlet  $L$  and non- $L$  functions: (Left to right)  $L(5,1)$  with regular zeros on  $x = 0$  as well as non-trivial zeros on  $x = \frac{1}{2}$ .  $L(5,2)$  with asymmetric non-trivial zeros on  $x = \frac{1}{2}$ .  $L(61,2)$  and  $L(666,1)$  similar to  $L(5,2)$  and  $L(5,1)$ . Right the period 10 non- $L$ -function with  $\chi = \{0,1,0,-1,0,0,0,1,0,-1\}$  (portrayed naked of any functional equation for 100 terms) has zeros in the critical strip  $0 < x < 1$  manifestly varying from the critical line, generated using the author's application RZViewer for Mac (<http://www.dhushara.com/DarkHeart/RZV/RZViewer.htm>).

In historical terms, there is a unique class of such series, which do appear to have their unreal zeros on the critical line - the Dirichlet  $L$ -series, or when extended to the complex plane,  $L$ -functions:

$$L(z, \chi) = \sum_{n=1}^{\infty} \chi(n) n^{-z} = \prod_{p \text{ prime}} (1 - \chi(p) p^{-z})^{-1} \text{ where } \chi(n), n = 0, \dots, k-1 \text{ is a Dirichlet character,}$$

It was originally proven by Dirichlet that  $L(1, \chi) \neq 0$  for all Dirichlet characters  $\chi$ , allowing him to establish his theorem on primes in arithmetic progressions.

A Dirichlet character is any function  $\chi$  from the integers to the complex numbers, such that:

- 1) **Periodic:** There exists a positive integer  $k$  such that  $\chi(n) = \chi(n+k)$  for all  $n$ .
- 2) **Relative primality:** If  $\gcd(n, k) > 1$  then  $\chi(n) = 0$ ; if  $\gcd(n, k) = 1$  then  $\chi(n) \neq 0$ .
- 3) **Completely multiplicative:**  $\chi(mn) = \chi(m)\chi(n)$  for all integers  $m$  and  $n$ .

Consequently  $\chi(1)=1$  and since only numbers relatively prime to  $k$  have non-zero characters, there are  $\phi(k)$  of these where  $\phi$  is the totient function, and each non-zero character is a  $\phi$ -th complex root of unity. These conditions lead to the possible characters being determined by the finite commutative groups of units in the quotient ring  $\mathbb{Z}/k\mathbb{Z}$ , the residue class of an integer  $n$  being the set of all integers congruent to  $n$  modulo  $k$ .

As a consequence of the particular definition of each  $\chi$ ,  $L(z, \chi)$  is also expressible as a product over a set of primes  $p_i$  with terms depending on the Dirichlet characters of  $p_i$ . As well as admitting an Euler product, the  $L$ -functions also have a generic functional equation enabling them to be extended to the entire complex plane minus a simple infinity at  $z = 1$  for the principal characters, whose non-zero terms are 1, as is the case of zeta.

Extending RH to the  $L$ -functions gives rise to the **generalized Riemann hypothesis** - that for all such functions, all zeros on the critical strip  $0 < x < 1$  lie on  $x = 1/2$ . Examining where the functional boundaries lie, beyond which the unreal zeros depart from the critical line, has become one major avenue of attempting to prove or disprove RH, as noted in Brian Conrey's (2003) review. Some of these involve considering wider classes of functions such as the  $L$ -functions associated with cubic curves, echoing Andre Weil's (1948) proving of RH for zeta-functions of (quadratic) function fields. Here, partly responding to Brian Conrey's claim of a conspiracy among abstract  $L$ -functions, we will restrict ourselves to the generalized RH in the standard complex function setting, to elucidate dynamic principles using Dirichlet series inside and outside the  $L$ -function framework.

## The Impossible Coincidence

To ensure convergence, zeta is expressed in terms of Dirichlet's eta function on the critical strip:

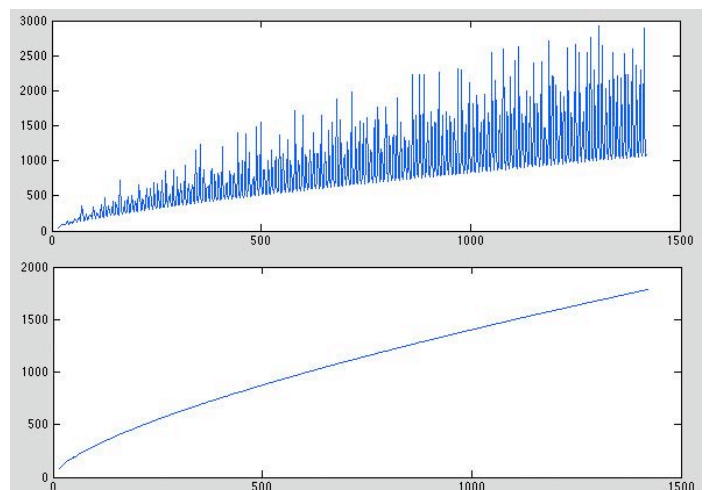
$$\zeta(z) = (1 - 2^{1-z})^{-1} \sum_{n=1}^{\infty} (-1)^{n+1} n^{-z} = (1 - 2^{1-z})^{-1} \eta(z) \text{ and then in terms of the functional equation}$$

$$\zeta(z) = 2^z \pi^{-1+z} \sin\left(\frac{\pi z}{2}\right) \Gamma(1-z) \zeta(1-z)$$

where  $\Gamma(z) = \int_0^{\infty} t^{z-1} e^{-t} dt$  in the half-plane  $\text{real}(z) \leq 0$ .

In terms of investigating the convergence of the series to its zeros, eta is better placed than zeta because the convergence is more uniform.

Fig 2: (Top) The number of iteration steps in the eta-derived zeta series required to get 5 steps with 0.005 of 0 varies erratically from one zero to the next, but this is a disguised effect of the presence of the  $1/(1-2^{1-z})$  term so becomes a smooth curve for eta (below).



RH is so appealing, as an object of possible proof, because of the obvious symmetry in all the zeroes lying on the same straight line, reinforced by Riemann's reflectivity relation:

$$\Gamma\left(\frac{z}{2}\right)\pi^{-\frac{z}{2}}\zeta(z) = \Gamma\left(1 - \frac{z}{2}\right)\pi^{-\frac{1-z}{2}}\zeta(1-z)$$

making it possible to express the zeros in terms of the function  $\xi(z) = \frac{1}{2}z(z-1)\Gamma\left(\frac{z}{2}\right)\pi^{-\frac{z}{2}}\zeta(z)$  for which  $\xi(z) = \xi(1-z)$ , so it is symmetric about  $x = 1/2$ , leading to any off-critical zeros of zeta being in symmetrical pairs. The function  $\Xi(z) = \Gamma\left(\frac{z}{2}\right)\pi^{-\frac{z}{2}}\zeta(z)$  also has this symmetry. It also applies to

the  $L$ -functions, for which:  $\xi(z, \chi) = \Gamma\left(\frac{z+a}{2}\right)(\pi/q)^{-\frac{z+a}{2}}L(z, \chi)$ ,  $a = \{\chi(-1) \equiv -1\}$ , with

$$i^a k^{1/2} \xi(z, \chi) = \sum_{n=1}^k \chi(n) e^{2\pi n i / k} \xi(1-z, \bar{\chi}).$$

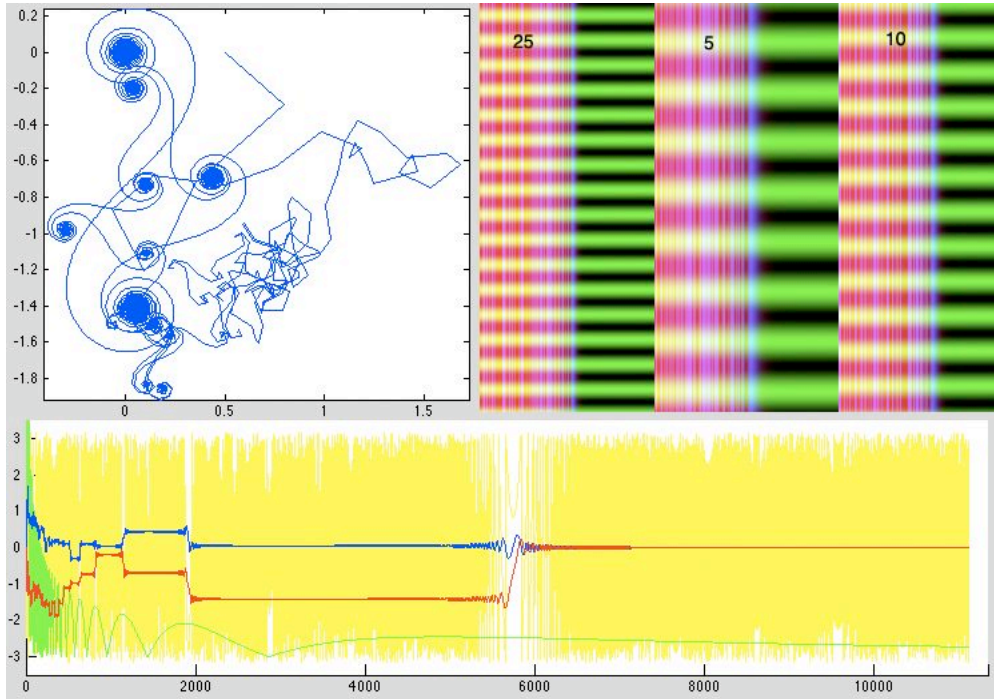


Fig 3: Top left sequence of iterates of eta for the 20,000<sup>th</sup> zero, showing winding into and out of a succession of spirals linking the real and imaginary parts of the iterates. Top right: The wave functions are logarithmic, leading to powers, but not multiples, having harmonic relationships. Below is shown the real and imaginary parts of the iterates (blue and red) overlaid on the absolute value and phase angle of individual terms (green and yellow). The zero is arrived at only after a long series of windings interrupted by short phases of mode-locking in the phases of successive terms.

However, when we come to examine the convergence in detail, this symmetry seems to be lost in the actual convergence process. Each term in the series for zeta is

$n^{-x+iy} = n^{-x}(\cos(y \ln n) + i \sin(y \ln n))$ , forming a series of superimposed logarithmic waves of

wavelength  $\lambda = \frac{2\pi}{\ln n}$ , with the amplitude varying with  $n^{-1/2}$  for points on the critical line. Unlike

power series, which generally have coefficients tending to zero,  $L$ -functions have coefficients all of absolute value 1, which means all the wave functions are contributing in equal amplitude in the sum except for the fact that the real part forms an index determining the absolute convergence. So RH is equivalent to all the zeros being at the same real (absolute) address.

The logarithmic variation means that the wave functions are harmonic only in powers, e.g. 5, 25, 125 etc. and not in multiples. This is reflected in both Riemann's primality proofs and other functions such as the Mobius function

$$\frac{1}{\zeta(z)} = \sum_{n=1}^{\infty} \frac{\mu(n)}{n^z}, \mu(n) = \begin{cases} (-1)^k, & n \text{ has } k \text{ distinct prime factors of multiplicity } 1 \\ 0 & \text{otherwise} \end{cases}. \text{ There is no manifest}$$

relationship between  $\ln n$  and  $n^{1/2}$  that explains why the zeros should be on  $x = 1/2$  and indeed we will find examples where they are not, so there is another factor involved - the primes.

The dynamics makes the uncomputability of this problem abundantly clear. If we take a given zero of eta, say the 20,000<sup>th</sup>, and plot the iterates, we find they wind into and out of a series of spirals associated with non-mode locked phases, where the angle of successive terms is rotating steadily, interrupted by briefer periods of phase locking, where the angles and hence the complex values of the iteration, make a systematic translation. Eventual convergence to zero occurs only after the last of these mode-locking episodes whose iteration numbers can be calculated directly, by finding where the waves match phase:

$$y \ln(n+1) = y \ln(n) + k\pi, \ln\left(\frac{n+1}{n}\right) = \frac{k\pi}{y}, 1 + \frac{1}{n} = e^{k\pi/y}, n = \frac{1}{e^{k\pi/y} - 1}.$$

This corresponds also to the mode shifts in the orbits in yellow and the series of maxima in green.

The product formula is no help in locating the zeros because it applies only for  $x > 1$  and, in the critical strip, it's multiplicative orbits are asymptotically unstable, with exponentially increasing fluctuations.

## Primes and Mediants - Equivalents of RH

Riemann developed an explicit formula for the prime counting function  $\pi(x)$  which is most easily expressed in terms of the related prime counting step function  $\psi(x) = \sum_{n \leq x} \Lambda(x)$ , the additive von

Mangoldt function, where  $\Lambda(x) = \log p$  if  $x = p^k$  and 0 otherwise. Notice here the exclusive appearance of prime powers eliminated in the Möbius function. We then have the explicit formula

$$\psi(x) = x - \sum_{\substack{\zeta(\rho)=0 \\ 0 < \text{Re}(\rho) < 1}} \frac{x^\rho}{\rho} - \frac{1}{2} \log(1 - x^{-2}) - \log(2\pi), \text{ where } \rho = 1/2 + it \text{ are the zeros of } \zeta(z), \text{ and the}$$

summation is over zeros of increasing  $|t|$ .

From Ingham (1932 83), we have  $\pi(x) = \text{li}(x) + O(x^\theta \ln x)$  where  $\theta = \sup_{\rho: \zeta(\rho)=0} (\text{real}(\rho))$ ,  $\text{li } x = \int_0^x \frac{dt}{\ln t}$ .

Hence the asymptotic behavior of the primes is determined by the real sup of the zeros. This comes about because the explicit formula shows the magnitude of the oscillations of primes around their expected position is controlled by the real parts of the zeros of the zeta function, since

$$\frac{x^\rho}{\rho} = \frac{e^{(p+iq)\ln(x)}}{p+iq} = \frac{x^p (\cos(q \ln x) + i \sin(q \ln x))}{p+iq} = \frac{x^p}{p^2 + q^2} (\cos(q \ln x) + i \sin(q \ln x))(p - iq)$$

$$\text{so } \frac{x^\rho}{\rho} + \frac{x^{\bar{\rho}}}{\bar{\rho}} = 2 \text{real}\left(\frac{x^\rho}{\rho}\right) = 2 \frac{x^p}{p^2 + q^2} (p \cos(q \ln x) + q \sin(q \ln x)) \sim 2 \frac{x^p}{p^2 + q^2} q \sin(\ln(x)q)$$

Hence RH has been shown to be equivalent to the statement  $|\pi(x) - \text{li}(x)| < x^{1/2} \log(x) / 8\pi$ .



A further equivalent of RH is that  $M(x) = \sum_{n \leq x} \mu(n) = O(x^{1/2+\varepsilon})$ , which would guarantee the Möbius function would converge for  $x > 1/2$ , and show there were no infinite poles (and hence no zeta zeros). A similar conjecture by Mertens that  $M(n) = \sum_{k=1}^n \mu(k) < n^{1/2}$ , which would have proved the Riemann hypothesis, was found false at a value of around  $10^{30}$  by Odysko's colleague Herman te Riele.

The Farey sequences appear in a third manifestation of RH (Franel and Landau 1924). These consist of all fractions with denominators up to  $n$  ranked in order of magnitude - for example,  $F_5 = \left\{ \frac{0}{1}, \frac{1}{5}, \frac{1}{4}, \frac{1}{3}, \frac{2}{5}, \frac{1}{2}, \frac{3}{5}, \frac{2}{3}, \frac{3}{4}, \frac{4}{5}, \frac{1}{1} \right\}$ . Each fraction is the mediant of its neighbours (i.e.  $\frac{n_1 + n_2}{d_1 + d_2}$ ).

In addition, for an adjacent pair  $\frac{a}{b}, \frac{c}{d}$ ,  $bc - ad = 1$ . Because the sequence of fractions removes degenerate common factors from the numerator and denominator, they are relatively prime and hence  $|F_n| = |F_{n-1}| + \phi(n)$  since  $F_n$  contains  $F_{n-1}$  plus all fractions  $\frac{p}{n}$  where  $p$  is coprime to  $n$ .

Two equivalents of RH state ([http://en.wikipedia.org/wiki/Farey\\_sequence](http://en.wikipedia.org/wiki/Farey_sequence)):

$$(i) \sum_{k=1}^{m_n} |d_{k,n}| = O(n^r), \text{ any } r > 1/2 \text{ and } (ii) \sum_{k=1}^{m_n} d_{k,n}^2 = O(n^r), \text{ any } r > -1$$

$$d_{k,n} = a_{k,n} - \frac{k}{m_n}, \text{ where } m_n \text{ is the length of the Farey sequence } \{a_{k,n}, k = 1, \dots, m_n\}$$

This is saying that the **Farey fractions are as evenly distributed as they can be** (to order  $n^{1/2}$ ) **given that they are by definition not evenly distributed [1]**, but determined by fractions with all (prime) common factors removed.

The same consideration applies to the asymptotic **distribution of the primes - they are as evenly distributed as they can be** (to order  $n^{1/2}$  from  $\text{li}(n)$ ) - **given that they are not evenly distributed [2]**, being those integers with no other factors.

This is reflected in other properties of the prime distribution, despite its manifest irregularity, reflected in such processes as the quadratic Ulam spiral. For example, the Dirichlet prime number theorem, states that there are infinitely many primes which are congruent to  $a$  modulo  $d$  in the arithmetic progression  $a+nd$ . Stronger forms of Dirichlet's theorem state that different arithmetic progressions with the same modulus have approximately the same proportions of primes. Equivalently, the primes are evenly distributed (asymptotically) among each congruence class modulo  $d$ .

What RH - that **the non-trivial zeros of the zeta function are all on the critical line [3]** - shows us is the order to which these fluctuations approach an even distribution is inverse quadratic because all the zeros appear to lie on  $x = 1/2$ . However the lack of a proof of RH suggests that these three statements are encoded forms of one another and that the locations of the zeros are a **consequence** of the distribution of primes rather than proving their asymptotic distribution, or at best that the three statements are encoded versions of one another. Thus RH is either true but unprovable except in finite numerical approximations, or a type of additional axiom like the axiom of choice that arises from infinities in calculation, just as the Collatz, and other discrete infinity problems appear to be versions of the undecidable Turing halting problem. Turing himself tried to prove computationally that RH was false! (Booker 2006).

We now turn to examining how a dynamical interpretation of the zeta zeros can explain why zeta and the Dirichlet  $L$ -functions have their non-trivial zeros on the critical line as a result of the asymptotically even distribution of the primes avoiding mode-locking which could knock the zeros 'off-line', as is the case for related functions where mode-locking is more pronounced.

## Mediants and Mode-Locking

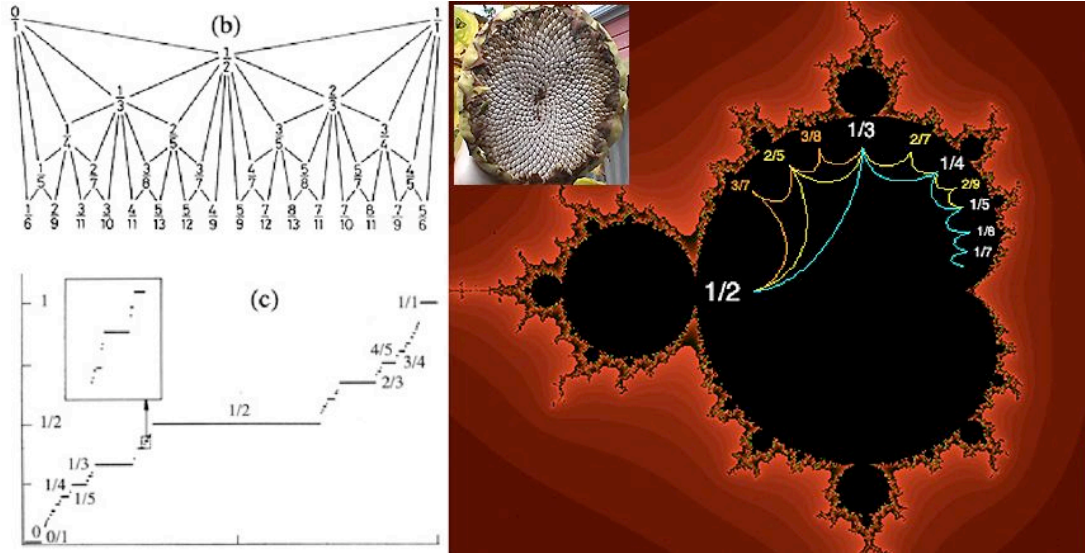


Fig 4: Left Farey Tree and Devils Staircase. Right: Mediant-based mode-locking in the Mandelbrot set bulbs, defining their fractional rotation, the periodicity in each bulb and the number of its dendrites - e.g.  $1/2$  and  $1/3$  span  $2/5$ . Spirals in the sunflower follow Fibonacci numbers, minimizing mode-locking by approximating the golden angle  $\gamma\pi$ .

In dynamical mode-locking, any irrational rotation close enough to a rational fraction of a revolution undergoing dynamical feedback becomes locked to the periodicity of that rotation, forming a series of intervals of mode-locked states, with a residual set of points in between retaining their unperturbed irrational motion. These mode locked intervals form a continuous fractal monotone increasing function, constant on intervals surrounding each rational number, called the Devil's staircase illustrated in fig 4. Mode-locking is manifest in many processes where dynamic periodicities interact, including the non-mode-locked orbits (to Jupiter) of the remaining asteroids, because the mode-locked ones were thrown into chaotic orbits and collided with planets, the ordered mode-locking of the Moon's day to the month, and Mercury's day to  $2/3$  of its year.

As shown in fig 4, the bulbs on the Mandelbrot set follow the fractions on the Farey tree, adding

fractions as mediants  $\frac{p}{q} + \frac{r}{s} = \frac{p+r}{q+s}$ . This can be seen by counting the number of their dendrites,

which also corresponds to the periodicity of the attractor in each bulb. Mediants correctly order the fractional rotations between 0 and 1 into an ascending Farey sequence, providing a way of finding the fraction with smallest denominator between any two other fractions. A way of seeing why this is so is provided by using a discrete process to represent the periodicities or fractional rotations. For example if we have  $2/3 = [110]$  and combine it with  $1/2 = [10]$  by alternating, we get  $[11010]$ , or  $3/5$ .

The Golden Mean  $\gamma = \frac{-1 \pm \sqrt{5}}{2} = 0.618, -1.618$ , by virtue of its defining relation  $\frac{1}{\gamma} = 1 + \gamma$  is the limit

of the ratios of successive Fibonacci numbers 1, 1, 2, 3, 5, 8, 13, 21 ... for which

$F_{n+1} = F_n + F_{n-1}$ ,  $F_0 = F_1 = 1$ , is non-mode-locked. The Farey tree leads to other Golden numbers, if we alternate left and right as we descend, following a series of Fibonacci fractions. Numbers  $g$ , such

as these, avoid becoming mode-locked because their distance from any fraction of a given denominator  $q$  exceeds a certain bound:  $\left|g - \frac{p}{q}\right| > \frac{\varepsilon}{q^2}$ ,  $\varepsilon \sim \frac{1}{\sqrt{5}}$ .

The golden numbers can most easily be described in terms of continued fractions, which, when truncated represent the closest approximation by rationals:  $n = a_0 + \frac{1}{a_1 + \frac{1}{a_2 + \frac{1}{\dots}}} = [a_0, a_1, a_2, \dots]$ .

Golden numbers end in a series of 1's thus having slower convergence to fractions of a given denominator than any other numbers. The Golden Mean itself is  $[1, 1, 1, \dots]$ . More generally, the Farey Tree has straightforward natural rules of parental and descendent inheritance, using continued fractions – e.g.  $2/5 = [2, 2] = [2, 1, 1]$  has descendents  $3/7 = [2, 3]$  and  $3/8 = [2, 1, 2]$  each gained by adding 1 to the last term in the two equivalent formulations. Any fraction or quadratic irrational has an eventually repeating continued fraction – e.g.  $1/\sqrt{3} = [1, \overline{2}]$ .

### A Mode-Locking View of the $L$ -functions and their Counterexamples

When we look at the sum formula for zeta, it appears to be simply a sum of powers of integers without the primes we see in the product formula, however, immediately we turn to zeta variants such as  $\frac{1}{\zeta(s)} = \sum_{n=1}^{\infty} \frac{\mu(n)}{n^s}$  and  $\frac{\zeta'(s)}{\zeta(s)} = -\sum_{n=1}^{\infty} \frac{\Lambda(n)}{n^s}$ , we see the primes reappearing the coefficients.

In the context of the natural numbers, the minimally mode-locked numbers are the primes, since the only common factor of a prime with any other number, apart from its own multiples, is 1. If we turn to the  $L$ -functions we see their characters are constructed to eliminate any form of mode locking in three distinct ways, while keeping all the non-zero contributions to the superimposed wave function of equal unit weight:

- (1) All coefficients of the bases not relatively prime to the period  $k$  are set to zero, leaving  $m = \phi(k)$  relatively prime coefficients.
- (2) The remaining coefficients of the relatively-prime bases are distributed cyclically with equally weighted values of absolute value 1 in the  $m$ -th roots of unity, according to a power of a generator of the  $m$  units of  $\mathbb{Z}/\mathbb{Z}k$ .
- (3) Since the group generators result in a sum that can also be represented as a product function over primes, the asymptotic distribution of primes places a final limit on any phase-locking.

The negation of the non-relatively prime bases is consistent with the removal of one or more

zeta/eta type series  $\sum_{n=1}^{\infty} (\pm 1)^{n-1} qn^{-z}$ ,  $q \nmid k$  for which RH applies, but the distribution around the

relatively prime residues with rotating coefficients arises from the group generators and the product representation, which again shows the primes becoming evident in the sum formula.

These conditions have been abstractly generalized into the four axioms of the so-called Selberg class, attempting to define the conditions which cause a Dirichlet series  $L(z)$  to have zeros on the critical line. These consist of:

- (1) Functional equation and (2) Euler product
- (3) Coefficients of order 1. Ramanujan conjecture  $a_1 = 1$ ,  $a_n \ll n^\varepsilon \forall \varepsilon > 0$ .
- (4) At most a single simple pole infinity at 1 i.e.  $(z-1)^m L(z)$  analytic for some  $m$ .

To assess the status of RH, we can thus consider a wider class of Dirichlet series functions, to see the effects of mode-locking of the wave functions in the critical strip. As a starting point we look at series where the coefficients are all 0 or roots of unity, but do not satisfy  $L$ -function conditions. Notice firstly that the only  $L$ -function solutions appear from the finite group theory to be periodic because the only characters of period  $kn$  consisting of characters in  $k$  are perfect periodic repeats of  $k$  characters and not cyclic, or fractal permutations. Non-primitive characters are likewise generated from homologies of the residue groups  $\chi_{kn}(p) = \chi_k(p \bmod k)$ ,  $\chi_{kn}(p) \neq 0$ .

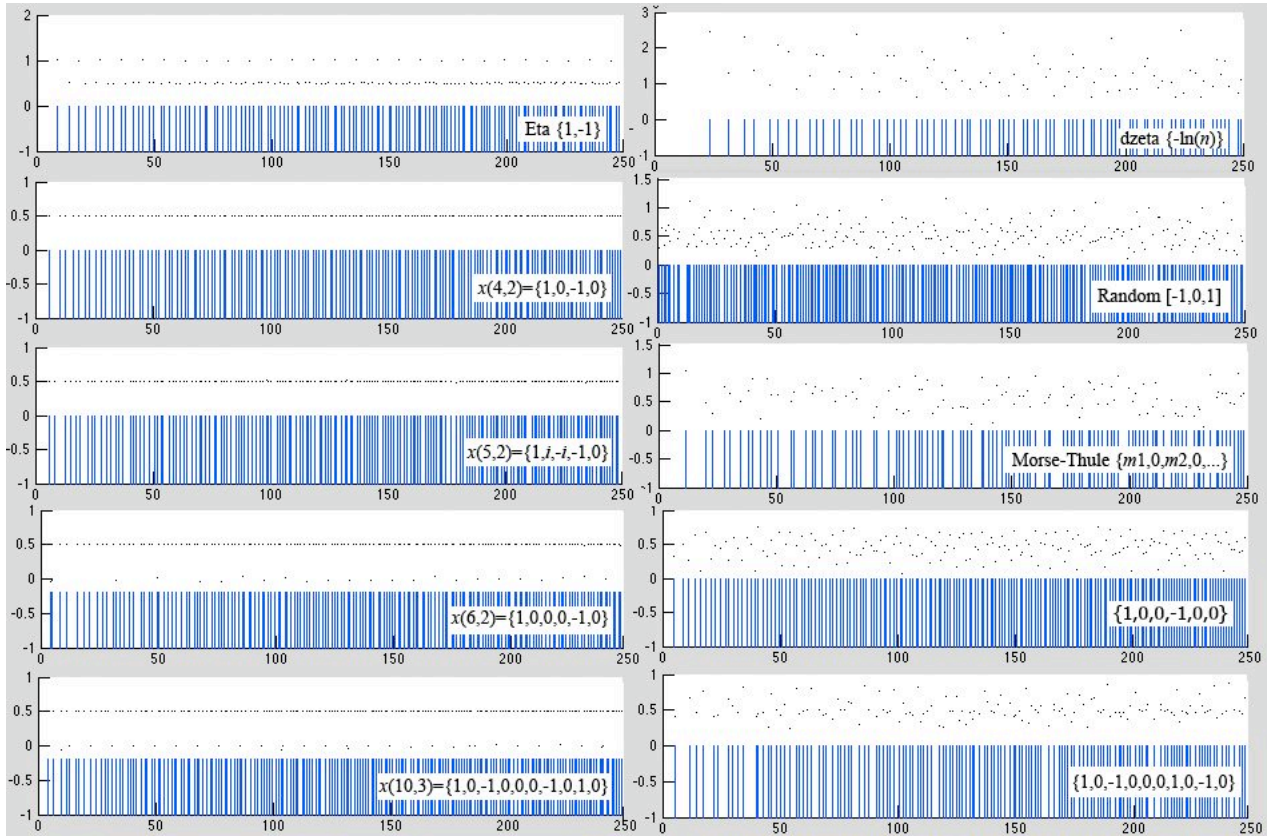


Fig 5: A series of  $L$ -functions and Eta (left) and RH-violating Dirichlet functions (right) whose critical strip zeros are illustrated by plotting their location (above) and their cumulative frequency, using a Matlab Newton's method scan.

In fig 5 on the left are shown the zeros of eta and a set of typical  $L$ -functions, confirming both the confinement of the zeros on  $0 < x < 1$  to  $x = \frac{1}{2}$ , and the  $t \ln(t)$  related cumulative frequency, discovered in Riemann's analysis of the zeta zeros. The method looks along a series of closely-spaced values running vertically for local absolute minima and then performs Newton's method using the approximate formal derivative for small  $h$ . On the right are shown a series of greater and lesser violations of the  $L$ -function / Selburg class conditions.

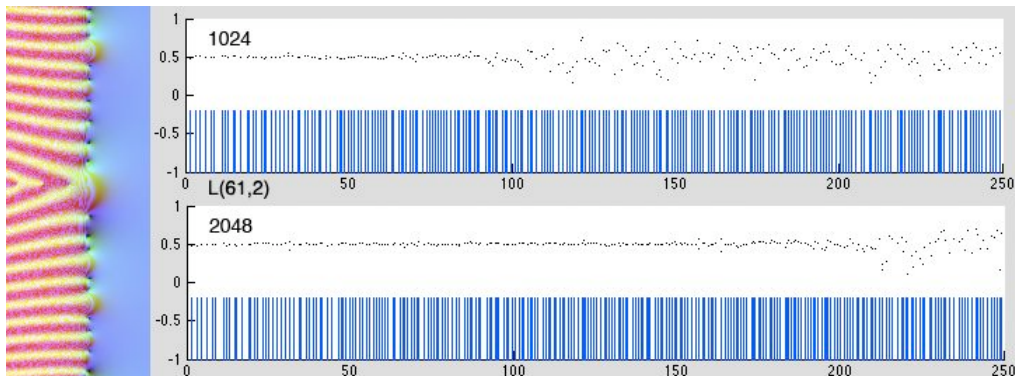


Fig 5b: Even with a confirmed  $L$ -function such as Dirichlet  $L(61,2)$  higher periods cause delayed convergence, requiring a disproportionate number of function terms to recognize zeros tending to the critical line.



From the top down we have the derivative of zeta  $\zeta'(z)$  by formal differentiation of the functional equation, which has terms effectively growing with  $-\ln(n)$ . Its zeros, corresponding to critical points of zeta, extend far out of the critical strip with an average real part of over 1. The next are Dirichlet series of random equi-distributed integers from  $\{-1, 0 \text{ and } 1\}$ . This shows zeros distributed with means close to  $x = \frac{1}{2}$ . Morse-Thule is a fractal sequence with even coefficients zero and the vector of odd coefficients recursively generated by  $v = [v, -v]$  with initial condition  $v = 1$  viz  $\{1, -1, -1, 1, -1, 1, 1, -1 \dots\}$  Again this has a mean close to  $x = \frac{1}{2}$ .

The last two are variants of the  $L$ -functions on their left by minor substitution. The first is effectively an alternating arithmetic series in 3's similar to that in 2's of  $\chi(4,2)$ , namely  $1^{-z} - 4^{-z} + 7^{-z} - \dots$ , showing arithmetic series of bases (or indeed any other sequence of coefficients) appear to have zeros on the critical line if and only if they correspond to  $L$ -functions. In particular these modified series are not necessarily completely multiplicative as the  $L$ -functions are leading to them not having a straightforward expression as an Euler product of primes, which might prevent phase-locking.

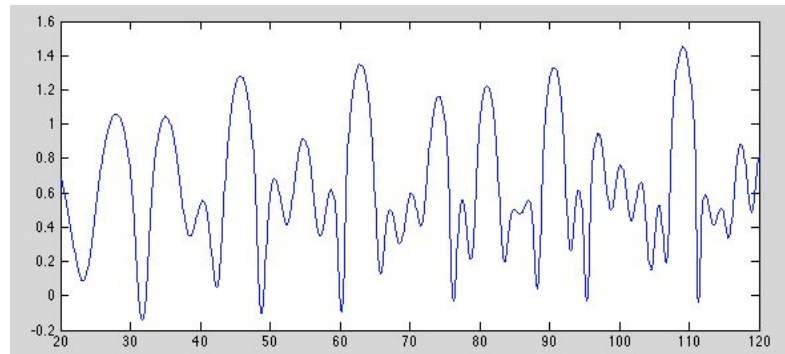
Function	Means over zeros in [0,1000]
Dzeta	1.1174
Random [-1,0,1]	0.5306, 0.4891, 0.4905
Morse-Thule $\pm\{0, +/-1, 0, +/-1\}$	0.5161
Golden Angle Rotation	0.6290
$\{1, 0, 0, -1, 0, 0\}$	0.4761
$\{1, 0, -1, 0, 0, 1, 0, -1, 0\}$	0.4959

Table 1: Some average  $x$  coordinates in the critical strip

From table 1 we can also see that, although these variants may have neither a functional equation nor an exact symmetry around the line  $x = \frac{1}{2}$ , the mean real value of their zeros still lie close to the critical line. This is also consistent with the average trends in zeta functions. For example, if we take the curve  $f(x) = 1 - \text{geometric mean}(\text{abs}(\zeta(x + iy) - 1))$ , we find it has a zero at  $\sim 0.5646$ .  
 $y=20\dots 120$  step 0.01

Fig 6: Function  $p(y)$  showing the  $x$ -coordinate for each  $y$ , where the absolute value of zeta differs by 1 from 1.

Alternatively when we take the individual curve  $p(y) = \{x : |\zeta(x + iy) - 1| = 1\}$  in the interval  $[20, 120]$ , as in fig 6, we find it has a geometric mean of 0.4965.



While these estimates are just very rough ad-hoc approximations because of the exponentiating irregularity of all these functions, they do indicate how zeros of Dirichlet functions can deviate significantly from the critical line while still having an averaged behavior closely spanning it. There is also no evidence for symmetric pairs of off-critical zeros, as would be required by the symmetry of the functional equations of zeta and the  $L$ -functions.

We still lack a broad spectrum of examples lying outside zeta and the Dirichlet  $L$ -functions where the zeros are on the critical line or its displaced equivalent. Classically all the examples found comprise more general types of zeta and  $L$ -functions where the coefficients are determined by more arcane primal relationships, essentially guaranteeing the zeros are on-line through more veiled

forms of primal non-phase-locking. In the following section we thus give a portrayal of the key types of abstract  $L$ -function, with a discussion of how their primal relationships arise.

### Widening the Horizon to other types of Zeta and $L$ -Function

To get a view of how  $L$ -functions can be extended beyond the context of Riemann and Dirichlet, a first stepping point is given by Dedekind zeta and Hecke  $L$ -functions of field extensions of the rationals  $\mathbf{Q}$  (Garrett 2011). Here we look for the non-zero ideals of the ring of integers in a field extension. These also share features of analytic continuation using functional equations and Euler products. Some such as  $\mathbf{Q}[\sqrt{5}]$  do not have unique prime factorizations and require consideration of the so-called class number.

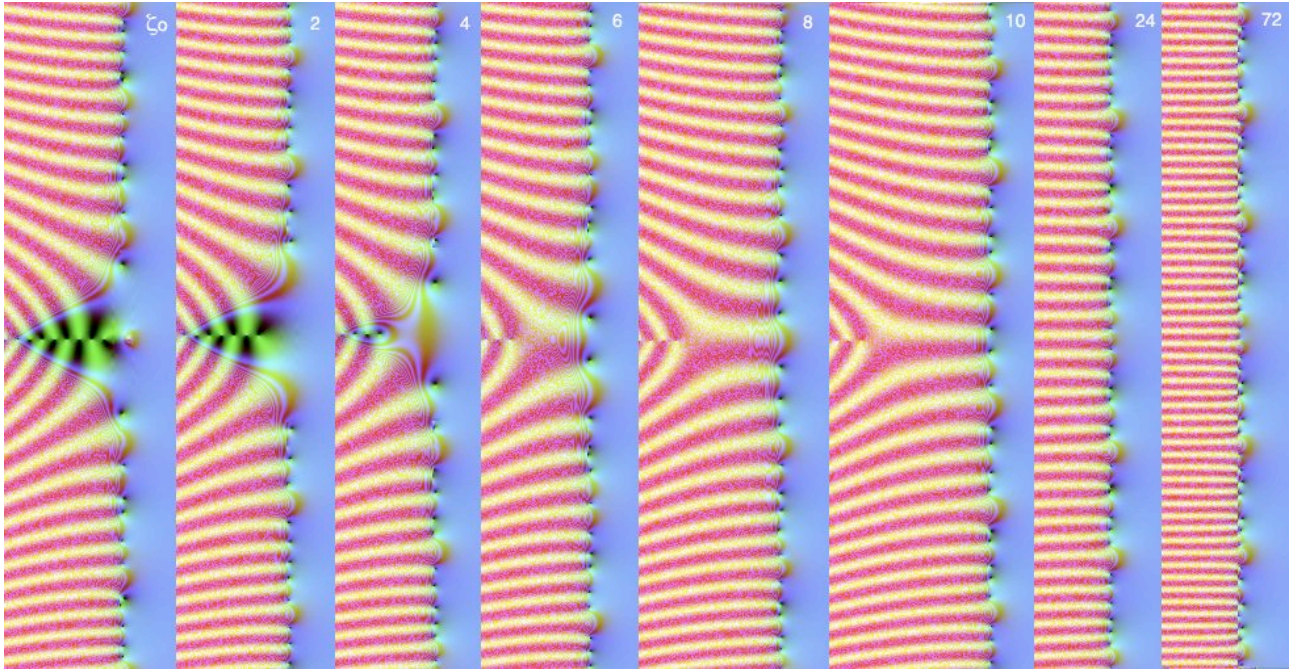


Fig 7: Profiles of the Dedekind zeta and Hecke  $L$ -functions for  $\mathbf{Z}[i]$ , the extension to the Gaussian integers. The portraits require both series representation, and the functional equation and Mellin transform theta integrals.

We will look at those of the Gaussian integers  $\mathbf{Z}[i]$ , defined by appending  $i$  to the integers, resulting in the lattice of complex numbers with integer real and imaginary parts. Here we have

$N\alpha = \alpha\bar{\alpha} = |\alpha|^2$ , so  $\zeta_o = \sum_{0 \neq \alpha \in \mathbf{o} \bmod \mathbf{o}^\times} \frac{1}{(N\alpha)^z} = \frac{1}{4} \sum_{m,n \text{ not both } 0} \frac{1}{(m^2 + n^2)^z}$ . This has a functional equation  $\pi^{-z}\Gamma(z)\zeta_o(z) = \pi^{-(1-z)}\Gamma(1-z)\zeta_o(1-z)$ , although, lacking an eta analogue, convergence isn't assured in the critical strip  $0 < x < 1$ , so Mellin integral transforms are commonly used to define the function more accurately there than is shown in fig 7, where the values in the critical strip have anomalies.

Correspondingly we have Hecke  $L$ -functions defined as follows. Consider the multiplicative group  $\chi: \mathbf{Z}[i] \rightarrow S^1$ ,  $\chi(\alpha) \rightarrow (\alpha/\bar{\alpha})^l$ ,  $l \in \mathbf{Z}$ . To give the same value on every generator this requires  $l$  to be trivial on units, hence  $1 = \chi(i) = \left(\frac{i}{-i}\right)^l = (-1)^l$ , so  $l \in 2\mathbf{Z}$ . We then have for each such  $l$  a Hecke

$L$ -function:  $L(z, \chi) = \sum_{0 \neq \alpha \in \mathbf{o} \bmod \mathbf{o}^\times} \frac{\chi(\alpha)}{(N\alpha)^z} = \frac{1}{4} \sum_{m,n \text{ not both } 0} \frac{(\alpha/\bar{\alpha})^l}{(m^2 + n^2)^z} = \prod_{\omega \text{ prime}} \frac{1}{1 - \chi(\omega)(N\omega)^{-z}}$  where the primes are now those of Gaussian integers, units  $\pm 1$  or  $\pm i$  times one of 3 types:  $1+i$  or a real prime which isn't a sum of squares ( $p \bmod 4 = 3$ ), or has coefficients squaring to a prime ( $p \bmod 4 = 1$ ).



Again we have a functional equation  $\pi^{-(z+|l|)}\Gamma(z+|l|)L(z,\chi)=(-1)^l\pi^{-(1-z+|l|)}\Gamma(1-z+|l|)L(1-z,\chi)$ .

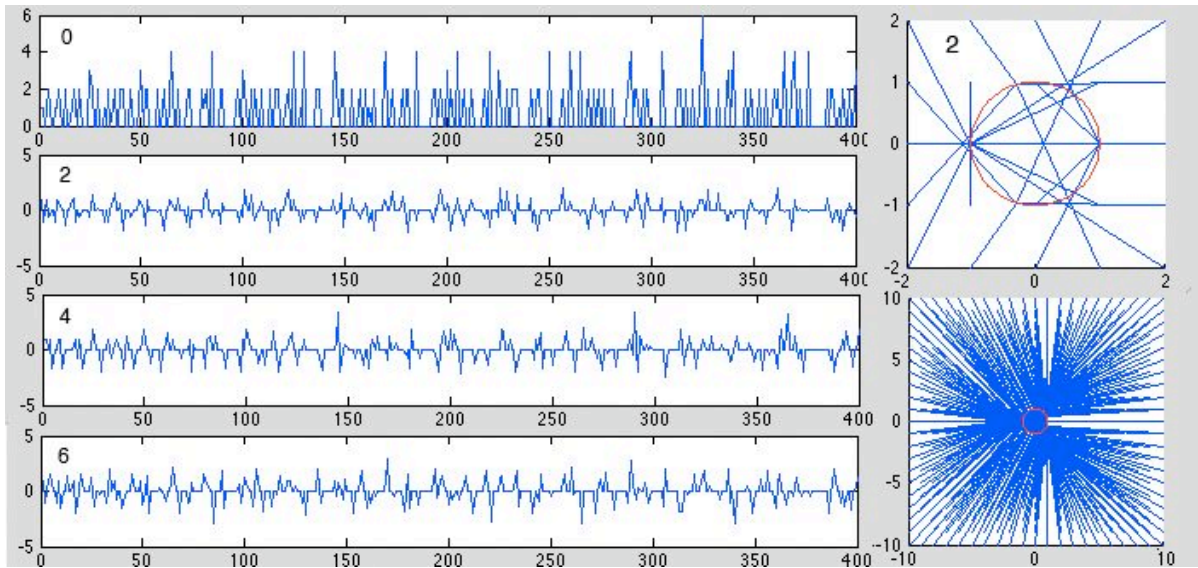


Fig 8: (Left) Profiles of the coefficients. Dedekind zeta (0) consists of the number of ways an integer can be represented as the sum of two integers divided by 4. The Hecke  $L$ -functions multiply these by the map  $\chi : Z[i] \rightarrow S^1$ ,  $\chi(\alpha) \rightarrow (\alpha / \bar{\alpha})^l$ ,  $l \in 2Z$  to the unit circle illustrated (right) for the case 2. Effectively this simply multiplies the angle of  $(m+in)$  by  $2l$  and sets the modulus to 1 since  $\chi(re^{i\theta}) = (e^{i\theta} / e^{-i\theta})^l = e^{2li\theta}$ ,  $l \in 2Z$ . It therefore plays a role similar to the Dirichlet characters in evenly distributing the coefficients.

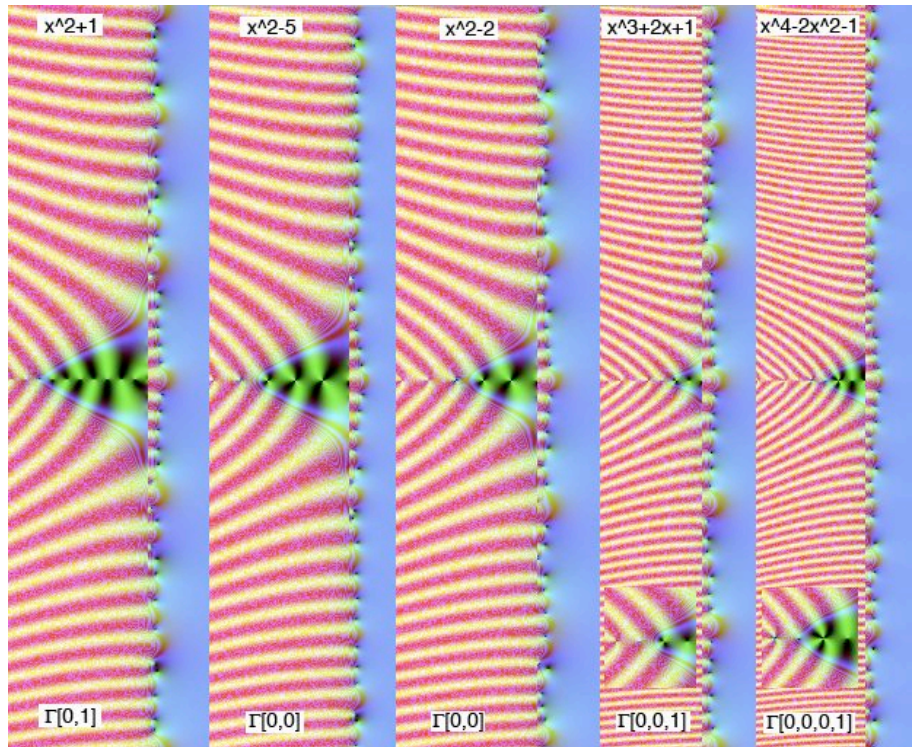
The profiles of these functions with their analytic continuations are shown in fig 7, requiring, in addition to the functional equations, use of Mellin transform integral formulae in the critical strip.

$$\zeta_o(z) = \pi^z \Gamma(z) \int_1^\infty (y^z + y^{1-z}) \frac{\theta(iy) - 1}{4y} dy, \quad \theta(iy) = \sum_{m,n \in Z} e^{-\pi(m^2+n^2)y} = \left( \sum_{n \in Z} e^{-\pi n^2 y} \right)^2$$

$$L(z, \chi) = \pi^{z+|l|} \Gamma(z+|l|) \int_1^\infty (y^z + (-1)^l y^{1-z}) \frac{\theta_\chi(iy)}{4y} dy, \quad \theta_\chi(iy) = \sum_{m,n \in Z} (m \pm in)^{2|l|} y^l e^{-\pi(m^2+n^2)y}$$

Fig 9: Dedekind zeta functions of a series of extension fields of polynomials portrayed with Dirichlet series and functional equation, but without the use of a Mellin transform in the critical strip, highlighting convergence failure of the Dirichlet series in the critical strip. Note the degenerate zeros in the left half plane caused by repeated gamma factors in the functional equation.

The theory of elliptic curves and modular forms also generate  $L$ -functions (Booker 2008), which involve Euler products with quadratic factors in the denominator.





In fig 10 are illustrated a variety of abstract  $L$ -functions from the genus-1  $L$ -function of the elliptic curve  $y^2 + y = x^3 - 7x + 6$ , through genus-2, 3 and 4 cases, to the  $L$ -function of a modular form based on the Ramanujan's Tau function using coefficients generated by PARI-GP using Tim Dokchitser's example files and Sage to generate elliptic equations from conductors (Dokchitser).

Hasse-Weil  $L$ -functions of elliptic curves  $E$  are generated by taking the function  $E(Q)$  over  $Q$ , or a field extension  $F$ , and estimating the number of rational points. Factoring mod  $p$  for primes  $p$  to get a set of  $A_p$  points on the curve  $E(F_p)$  up to a maximum of  $p+1$ . We then let  $a_p = p+1 - A_p$  the number of missing points. For each  $p$  we define:

$$L(E, z) = \sum_{n=1}^{\infty} a_n n^{-z} = \prod L_p(E, z), \quad L_p(E, z) = \begin{cases} 1 - a_p p^{-z} + p^{1-2z} & \text{good reduction} \\ 1 - a_p p^{-z} & \text{bad reduction} \end{cases}$$

Where bad reduction i.e. a singularity of  $E(F_p)$  results from repeated roots in  $F_p$ , in which case  $a_p = \pm 1$  depending on the splitting of the multiplicative reduction ( $p|N$  but not  $p^2$ ) of  $E$ , or is 0 if  $p^2|N$ .

The Birch and Swinnerton-Dyer conjecture asserts that the rank of the abelian group  $E(F)$  of points of  $E$  is the order of the zero of  $L(E, z)$  at  $z = 1$ . If  $L^*(E, z) = N^{z/2} (2\pi)^{-z} \Gamma(z) L(E, z)$ , then

$L^*(E, z) = \varepsilon L^*(E, 2-z)$ , where  $N$  is the conductor, the product of bad primes, and  $\varepsilon = \pm 1$ .

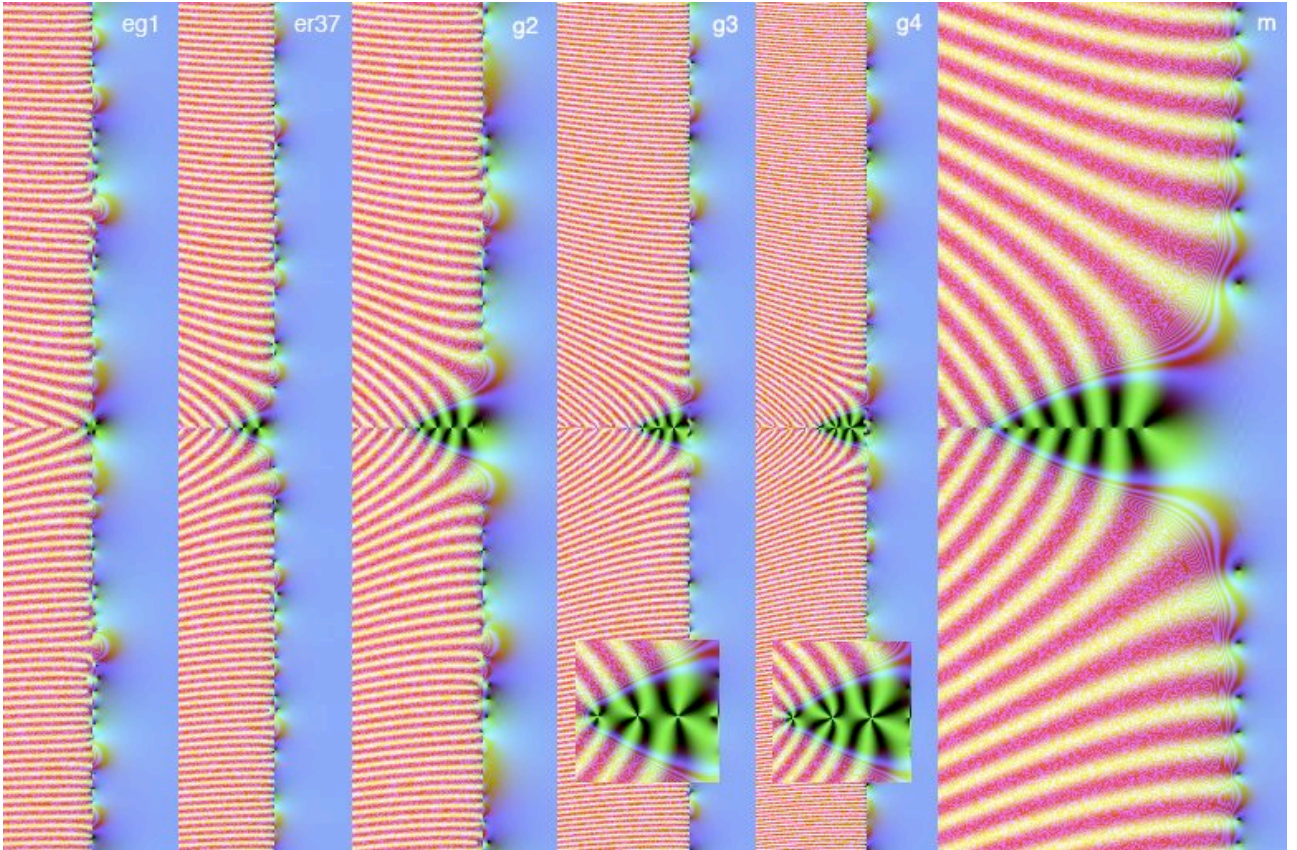


Fig 10: From left to right,  $L$ -functions of the genus-1 elliptic curve  $y^2 + y = x^3 - 7x + 6$ , the elliptic curve  $y^2 + y = x^3 + 2x^2 + (19 + 8\omega)x + (28 + 11\omega)$ ,  $\omega = (1 + \sqrt{37}) / 2$  over  $K = \mathbb{Q}(\sqrt{37})$ , the genus-2 curve  $y^2 + (x^3 + x + 1)y = x^5 + x^4$ , the genus-3 curve  $y^2 + (x^3 + x^2 + x + 1)y = x^7 + 2x^6 + 2x^5 + x^4$ , the genus-4 curve  $y^2 + (x^5 + x + 1)y = x^7 - x^6 + x^4$ , and the modular cusp form  $\Delta(z) = \sum_{n \geq 1} \tau(n) e^{2\pi i n z}$ ,

of weight 12, the ‘modular discriminant’, using Ramanujan's Tau function

$$\tau(n) = (5\sigma(n, 3) + 7\sigma(n, 5)) \frac{n}{12} - 35 \sum_{k=1}^{n-1} (6k - 4(n-k)) \sigma(k, 3) \sigma(n-k, 5), \quad \text{where } \sigma(n, k) = \sum_{d|n} d^k.$$



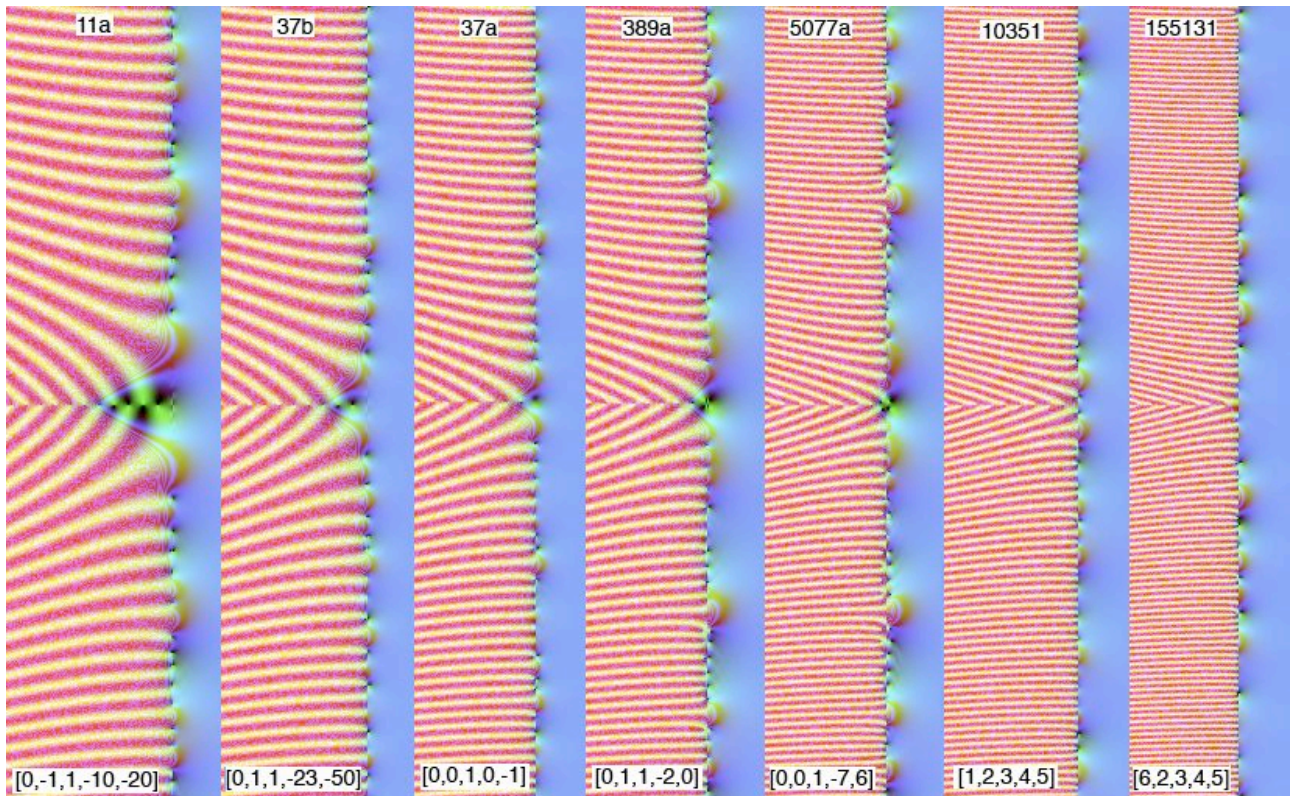
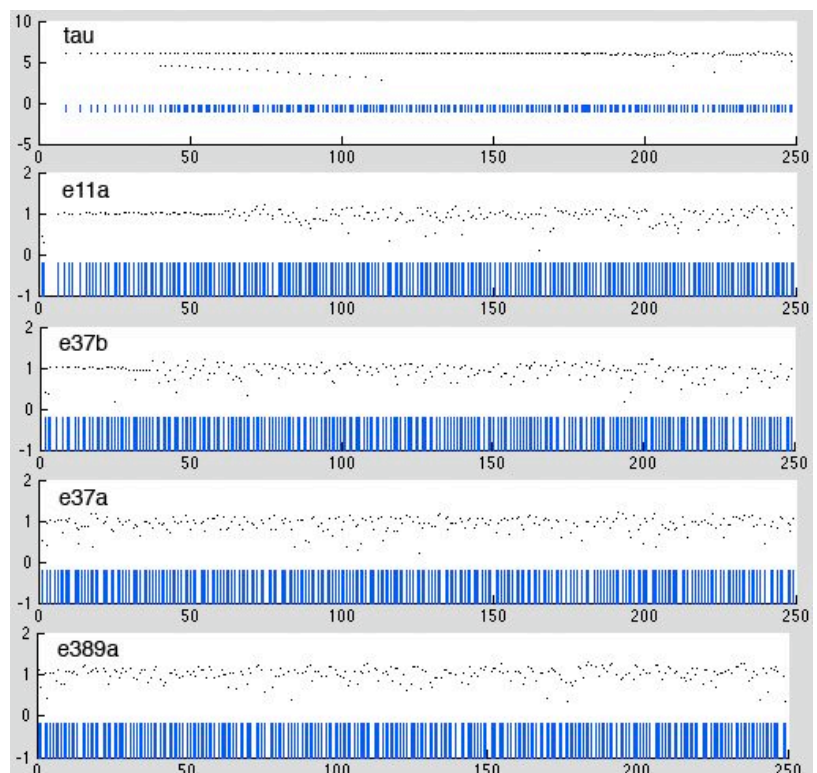


Fig 10b: A menagerie of  $L$ -functions of elliptic curves over  $\mathbb{Q}$  classified by their conductors (above) and their defining equations (below) where  $[a,b,c,d,e]$  corresponds to  $y^2 + axy + cy = x^3 + bx^2 + dx + e$

Although the function depends on a rather arcane definition through an elliptic curve and then a quadratic Euler product, the resulting Dirichlet series is a standard sequence of coefficients, which possesses a standard functional equation and can thus be portrayed as a meromorphic function in  $\mathbb{C}$  (analytic except for a finite number of simple infinities). For example for the elliptic curve above, the first few coefficients are:  $\{1, -2, -3, 2, -4, 6, -4, 0, 6, 8, -6, -6, -4, 8, 12, -4, -4, -12, -7, -8, \dots\}$ .

Fig 10c: Newton's method on the Dirichlet series representation at 1000 terms for the modular form Delta and four elliptic curves of lowest conductor, in fig 10b, show convergence to the critical line, for smaller imaginary values, similar to that of fig 5b for the Dirichlet  $L$ -function  $L(61, 2)$ , with convergence diminishing, as the conductor becomes larger. Tim Dokchitser's Computel, now in Sage can give a more accurate numerical calculation for individual zeros using Mellin transforms.

Elliptic functions over  $\mathbb{C}$  are genus-1 curves topologically equivalent to embeddings of a torus in  $\mathbb{P}^1 \times \mathbb{P}^1$  where  $\mathbb{P}^1$  is the complex projective plane or Riemann sphere derived by adding a single point at  $\infty$  to  $\mathbb{C}$ . Higher degree curves can



generate higher genus examples, as illustrated in fig 10.

Complementing the  $L$ -functions of elliptic curves are those of modular forms. The toroidal nature of the elliptic function results in it being periodic on a parallelogram in  $C$ . This results in a deep relationship with another kind of  $L$ -function. A modular function is a meromorphic function in the upper half-plane which is conserved by the modular group i.e.  $f(az+b)/(cz+d)=f(z)$ . More generally we have modular of weight  $w$  (necessarily even) if  $f(az+b)/(cz+d)=(cz+d)^w f(z)$ . If it is analytic in the upper half-plane we say it is a *modular form*.

Since  $f(z+1)=f(z)$   $f$  is periodic, we have a Fourier expansion  $f(z)=\sum_{n=0}^{\infty} a_n e^{2\pi i n z}$  and using the Mellin

transform  $M(f,z)=\int_0^{\infty} f(t)t^{z-1}dt$ , we can derive the  $L$ -function

$$L(f,z)=(2\pi)^2 M(f,z)/\Gamma(z)=\sum_{n=1}^{\infty} a_n n^{-z} \text{ which again has a functional equation. If}$$

$$L^*(f,z)=N^{z/2}(2\pi)^{-z}\Gamma(z)L(f,z), \text{ then } L^*(f,z)=(-1)^{w/2}L^*(E,w-z), \text{ and } L^* \text{ is meromorphic on } C.$$

In the case of weight  $w=2$  there is thus a correspondence between the functional equations of elliptic curves and modular forms. The Taniyama-Shimura conjecture asserts that every elliptic curve over  $\mathbb{Q}$  has a modular form parametrization, essentially through the periodicities induced by its toroidal embedding, a relationship pivotal in the proof of Fermat's last theorem (Daney).

Each of the types of  $L$ -function discussed admit a functional equation determined by the Dirichlet series, a number of gamma factors the conductor, and a sign a sign factor:

$$L^*(f,z)=N^{z/2}(2\pi)^{-z}\Gamma\left(\frac{z+\lambda_1}{2}\right)\dots\Gamma\left(\frac{z+\lambda_d}{2}\right)L(f,z), \text{ then } L^*(f,z)=\varepsilon L^*(E,w-z)$$

where  $|\varepsilon|=1$ ,  $\varepsilon=e^{2\pi i k/n}$  for Dirichlet  $L$ -functions  $\varepsilon=\pm 1$  otherwise.

The general Langlands philosophy includes a comparable explanation of the connection of polynomials of degree  $m$ . For a new type of degree 3  $L$ -function see (Booker 2008).

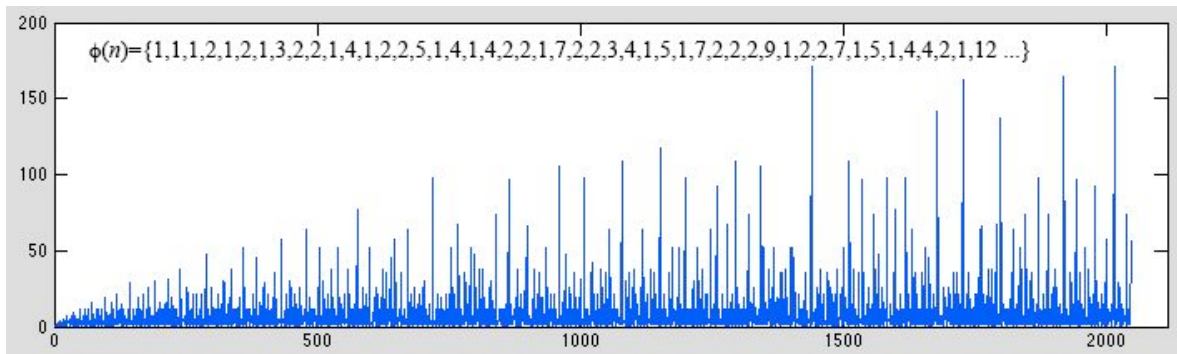


Fig 11: Unordered factorizations as a function of  $n$ .

## Seeking Examples with Product Formulae

The difficulty with our current set of examples is that all the  $L$ -functions have their critical strip zeros on the critical line and all the other functions we have looked at lack ostensible product representations. We now explore functions that do have a product representation to seek further examples outside the class of  $L$ -functions.



Let us consider the product of integers:

$$f(x) = \prod_{n=2}^{\infty} (1 - n^{-z})^{-1} = \sum_{n=1}^{\infty} \phi(n) n^{-z}, \quad \phi(n) = \text{unordered factorizations of } n.$$

The ‘unordered’ factorizations (in which different orders are not distinct) consist of all possible distinct  $n^{-z}$  terms in the product, which become coefficients of a given  $n$ . For example for 12 we have 4: 12, 6.2, 4.3, 3.2.2, written in descending order of the factors involved. With zeta and the  $L$ -functions, because prime factorization is unique, there is only one such term, so the coefficients of zeta are all 1. In this case, the coefficients vary widely, according to the distribution shown in fig 11, and we will expect to see significant phase-locking in the imaginary waves.

The number of unordered factorizations of  $n$  with largest part at most  $m$  can be calculated from the recursion relation  $\phi(m, n) = \sum_{\substack{d \mid n \\ d \leq m}} \phi(d, n/d)$  (Hughes & Shallit 1983, Knopfmacher & Mays 2006).

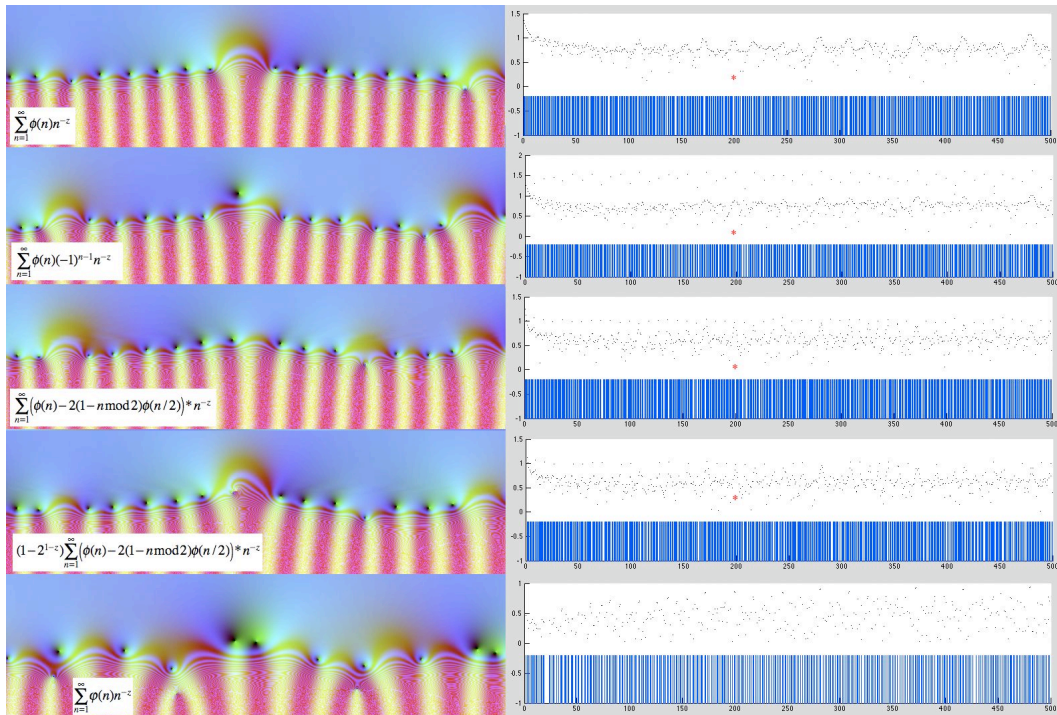


Fig 12: Dirichlet functions derived from an integer rather than a prime product show evidence of phase locking arising from their erratically increasing coefficients. Left naked plots in the region of 200, starred at the right where Newton’s method is used to seek for zeros. All are at 1024 series terms except the bottom pair at 250 terms.

To give an exploratory profile based on alternating series, we examine the related functions:

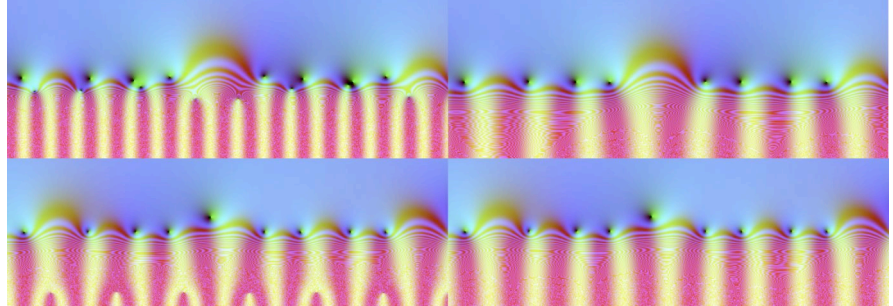
$\sum_{n=1}^{\infty} \phi(n) (-1)^{n-1} n^{-z}$ , the alternating variant, the function  $\sum_{n=1}^{\infty} (\phi(n) - 2(1 - n \bmod 2) \phi(n/2)) * n^{-z}$  which is derived from that of  $f(x)$  in the same way as eta is derived from zeta by subtracting  $2^{1-z}$  times the series from itself, and  $(1 - 2^{1-z})^{-1} \sum_{n=1}^{\infty} (\phi(n) - 2(1 - n \bmod 2) \phi(n/2)) * n^{-z}$ , the zeta series re-derived from the previous alternating series. We also for a comparison investigated the series

$$f_{-}(x) = \prod_{n=2}^{\infty} (1 + n^{-z})^{-1} = \sum_{n=1}^{\infty} \varphi(n) n^{-z}, \quad \varphi(n) = \text{unordered factorizations of } n \text{ with alternating powers,}$$

viz  $\{1, -1, -1, 0, -1, 0, -1, -1, 0, 0, -1, 0, -1, 0, 0, 1, -1, 0, -1, 0, 0, 0, -1, 1, 0, 0, -1, 0, -1, 1, -1, -1, 0, 0, 0, 1 \dots\}$  calculated by sorting factorizations into bins, removing duplicates and checking against the above method.

As can be seen from fig 12, both the Newton's method Matlab portrait and the function plot using the software application developed by the author (see below) show quasi-regular variations in the position of the zeros, consistent with substantial phase-locking caused by the fluctuating (repeated) coefficients. The two representations of the factorization zeta function top and second bottom show a degree of consistency, which can be compared with the naked and analytic versions of zeta itself in fig 13. By contrast, the last pair, which end up having quasi-random coefficients close to 0, 1 and -1, the portrait is similar to the random coefficient Dirichlet sequence of fig 5.

Fig 13: Naked and analytic portraits of zeta (above) and eta (below) show that eta's alternating series naked representation is true to its equivalent representation analytically in the critical strip, while zeta's shows distortions of the zeros caused by non-convergence of the absolute series.



We now examine more closely how Euler products of primes with varying coefficients might fare when encoded back into Dirichlet series. We can't take the products directly because these are unstable in the critical strip, and each involves an infinite number of terms in the sum, however, if we define a set of coefficients  $\chi(p)$  for each prime then we have for each term

$$\frac{1}{1 - \chi(p)p^{-z}} = \sum_{n=0}^{\infty} (\chi(p)p^{-z})^n = 1 + \chi(p)p^{-z} + (\chi(p))^2(p^2)^{-z} + \dots$$

and since each base  $n$  in the sum

has a unique prime factorization  $n = p_1^{m_1} \dots p_k^{m_k}$  it will have a uniquely-defined sum coefficient  $\chi(n) = (\chi(p_1))^{m_1} \dots (\chi(p_k))^{m_k}$ . Any such coefficient set is completely multiplicative as  $L$ -function characters are. More generally we could define  $\chi(p, n)$  separately for each  $p^n$ , which would be multiplicative, but not completely.

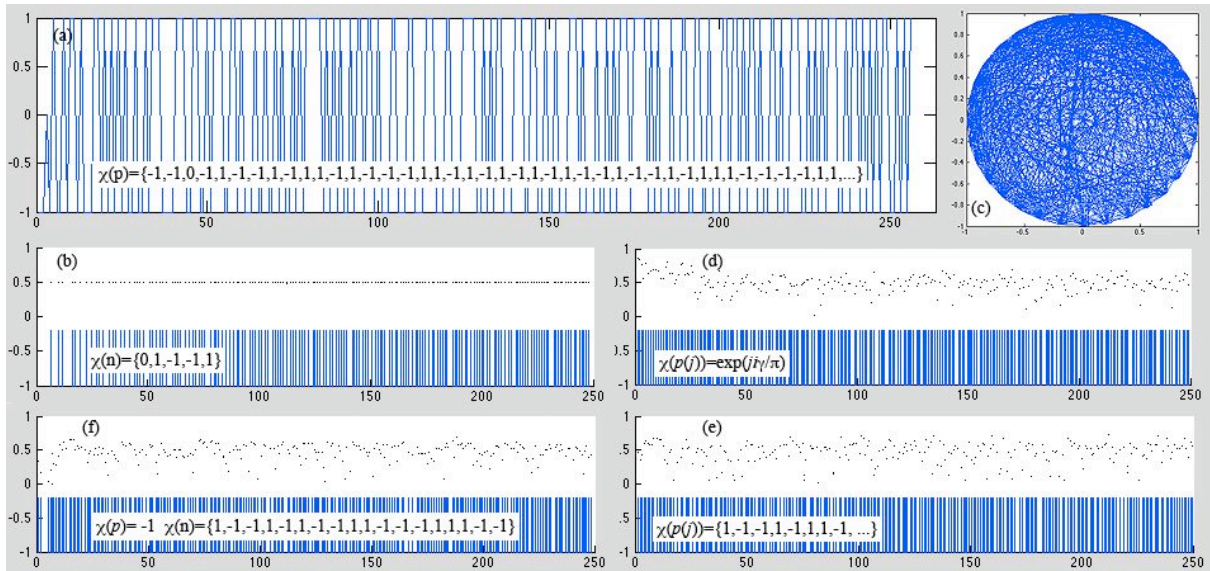


Fig 14: (a) The multiplicative coefficients of  $L(5,3)$  (b) form an irregular distribution on the primes (d) a golden mean angle variation on the prime product coefficients (c) and a Morse-Thule fractal recursive distribution of  $\{1,-1\}$  have zeros off the critical line, with significant indications of phase-locking as does the lambda function (f) with all prime multiplicative coefficients -1, but this function does have zeros on the critical line  $x=1/4$  through its analytic expression in terms of zeta indicating lack of convergence of the naked approximation.

In fig 14 are shown a set of examples where similar variations of the completely multiplicative coefficients have been chosen to those of the additive coefficients in fig 5. In all cases apart from



(b) the zeros are distributed off the critical line, showing an Euler product is not sufficient to cause the zeros to be on the critical line.

This brings us to a major caveat about representing approximations as naked functions in the 'forbidden' zone  $x < 0$ .

The lambda function  $\sum_{n=1}^{\infty} \frac{\lambda(n)}{n^s} = \prod_{p \text{ prime}} (1 + p^{-s})^{-1}$ , where  $\lambda(n) = (-1)^{\Omega(n)}$   $\Omega(n)$ = number of prime factors of  $n$  with multiplicity, as shown in fig 14(f), has multiplicative coefficients  $\chi(p) = -1$ , and can immediately be expressed in terms of the zeta function, since  $\frac{\prod_{p \text{ prime}} (1 - p^{-s})}{\prod_{p \text{ prime}} (1 - (p^2)^{-s})} = \frac{\zeta(2s)}{\zeta(s)}$ .

However the naked function is only marginally similar to its analytic continuation as shown in fig 15 (left) which has zeros on the line  $x = 1/4$  and singularities at the position of the zeta zeros, which are barely expressed at 1024 naked function terms.

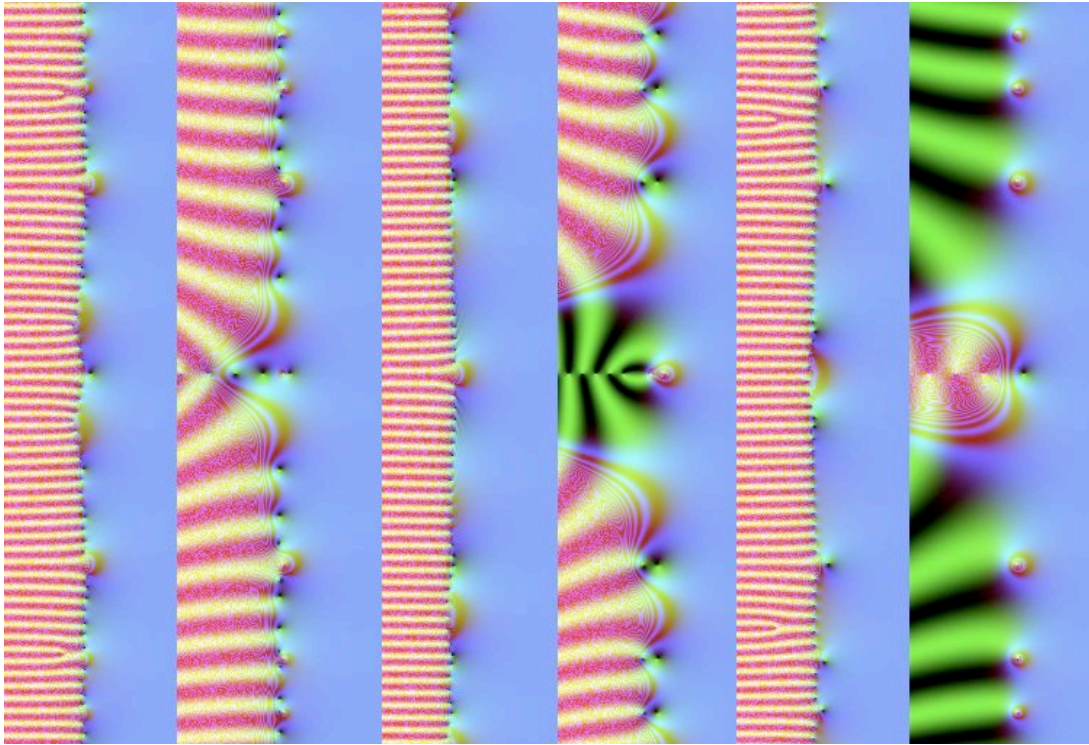


Fig 15: Failure of adequate convergence to the analytic continuation in lambda (left 2) sigma (centre 2) and mu (right 2) at 1024 function terms.

Even more pertinently, the two other derived functions sigma and mu have naked approximations with a very low degree of convergence to their analytic continuations.

Sigma  $\sum_{n=1}^{\infty} \frac{\sigma(n)}{n^s} = \zeta(s)\zeta(s-1)$ ,  $\sigma(n) = \sum_{d|n} d$  is defined in terms of the divisor function and is equivalent to a product of zetas. As shown centre in fig 15 its features and double zeros are barely apparent at 1024 terms.

Finally (right) we have mu,  $\sum_{n=1}^{\infty} \frac{\mu(n)}{n^s}$ ,  $\mu(n) = \begin{cases} (-1)^k, & n \text{ has } k \text{ distinct prime factors of multiplicity 1} \\ 0 & \text{otherwise} \end{cases}$

Which, from convolutions  $\sum_{n=1}^{\infty} \frac{f(n)}{n^s} \sum_{n=1}^{\infty} \frac{g(n)}{n^s} = \sum_{n=1}^{\infty} \frac{(f * g)(n)}{n^s}$ , where  $(f * g)(n) = \sum_{d|n} f(d)g(n/d)$  resolves to  $\sum_{n=1}^{\infty} \frac{\mu(n)}{n^s} = \frac{1}{\zeta(s)}$ , since  $\frac{1}{\zeta(s)} \zeta(s) = 1$ , and  $\mu * 1 = \varepsilon$ ,  $\varepsilon(n) = \begin{cases} 1, & n = 1 \\ 0, & n > 1 \end{cases}$ . Consequently this has Euler product  $\sum_{n=1}^{\infty} \frac{\mu(n)}{n^s} = \prod_{p \text{ prime}} (1 - p^{-s})$ .

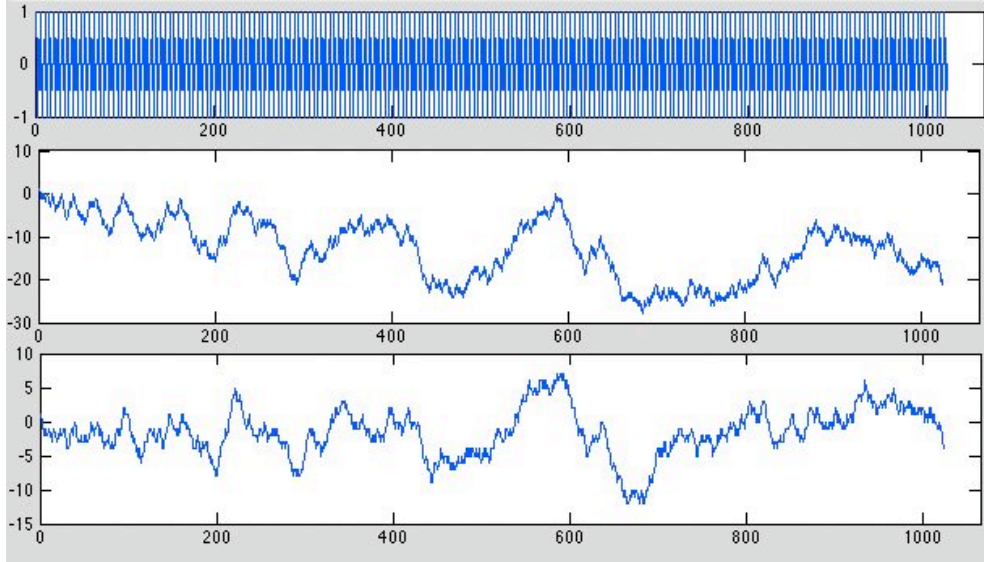


Fig 16: Trends in the added coefficients are emphasized when they are summed.  $L(5,3)$  has stable periodic sums, while lambda and mu have erratic long-term trends, which disrupt their convergence in the critical strip when calculated raw.

Fig 16 shows why convergence is bad for sigma and mu, which, unlike eta and the  $L$ -functions of non-trivial Dirichlet characters, illustrated by  $L(5,2)$  which have regularly alternating sum coefficients, have coefficients with large amounts of drift to the positive and negative, compromising their convergence. Many series generated from simple or cyclic multiplicative coefficients share such irregularities in the sum coefficients because of their varied impact on each integer through its prime factorization.

Ideally one would like an eta analogue to guarantee convergence of these functions in the critical strip, however solutions such as applying additional product terms to zeta \* lambda for each +1 and -1 coefficient for real multiplicative coefficients produces spurious functions with zeros on  $x = 0$  and  $x = 1/4$ , displaying the failure of convergence that occurs with the Euler product itself.

Alternatively, as we have seen with the Dedekind zeta and Hecke  $L$ -functions, is to represent the function in the critical strip, or even more widely, using a Mellin integral transform representation. However finding a suitable theta function can prove problematic. Tim Dokchitser's Computel PARI script, now incorporated into Sage uses just such a sophisticated Mellin technique to explore a variety of abstract  $L$ -functions.

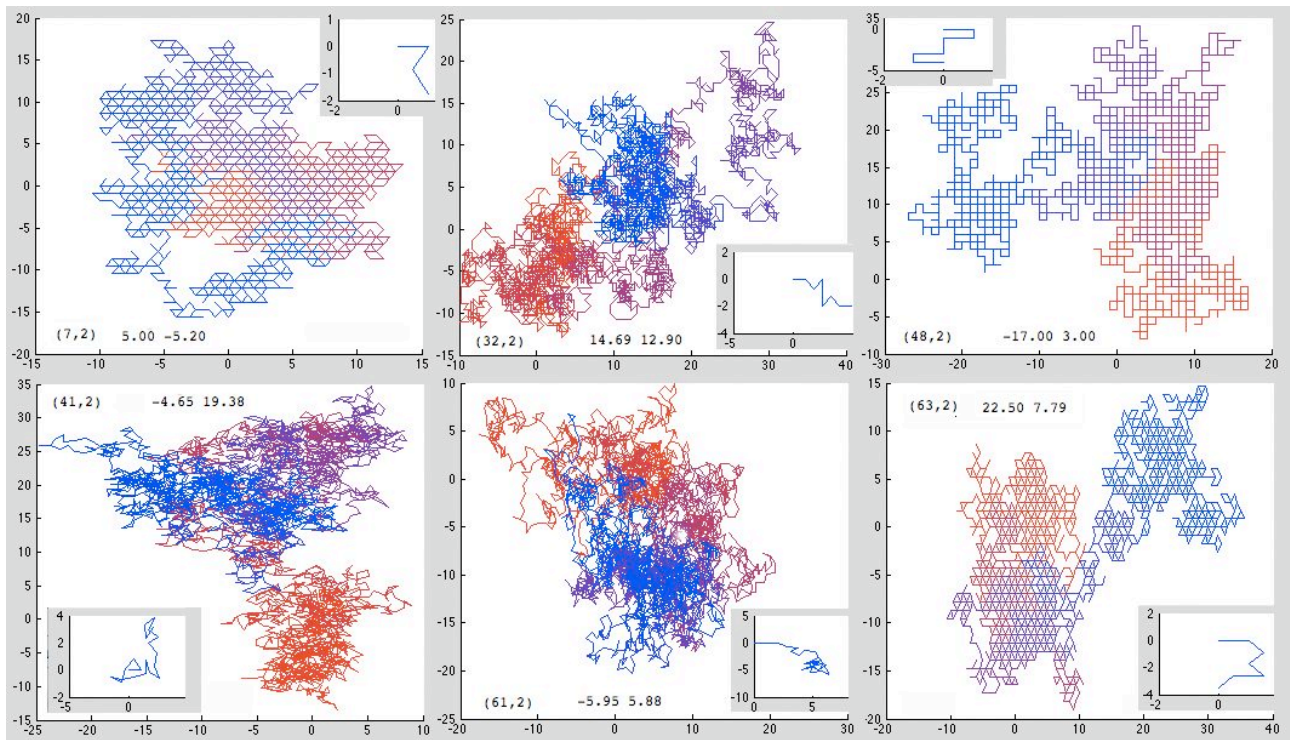


Fig 17: Trends in the multiplicative coefficients, emphasized by summing terms, are complex, even for Dirichlet  $L$ -functions, where the sum coefficients are strictly periodic (inset). The coefficient chain proceeds from red to blue.

Conversely, turning to the multiplicative coefficients, we see that it is no easy task to find criteria here which distinguish  $L$ -functions apparently satisfying RH from completely multiplicative functions which violate it, because the multiplicative coefficients for simple periodic Dirichlet series are encrypted through the primes into complex irregular sequences, with Brownian-like drift in their summed terms, as illustrated for a series of  $L$ -functions in fig 17.

### Dynamically Manipulating the Non-trivial Zeros in and out of the ‘Forbidden Zone’

To get a closer view of the dynamics of the zeros we now investigate breaking out of the boundaries imposed both by the  $L$ -functions and the taboos created by the assumption that Dirichlet functions can be depicted for negative real parts only if they have a formal functional equation. We will thus continue to ‘unashamedly’ use a ‘naked’ depiction of Dirichlet series in the ‘forbidden zone’, particularly those containing alternating terms, without exerting any functional equation, or expecting complete multiplicativity, so that we can see the dynamics of how zeros of such functions change under a continuous transformation between  $L$ -functions. Since we are actually using finite approximations, the functions we visualize will all be tame approximations, since for relatively small imaginary values in the tens to hundreds, no more than a few hundred terms of the Dirichlet series are needed to get a good approximation in these cases, which clearly show zeros on the line for the naked equivalents of these  $L$ -functions because of their convergence in the critical strip.

We will view how both changes in the character cast of  $L$ -functions and changes in which the usual integer values of the base exponents may be continuously shifted to adjacent real and complex values, to enable a continuous transformation between differing integer values.

Rather than attempting a one-process solution to the dynamics, our aim is to explore emergent features of the dynamics of zeros under such continuous transformations of Dirichlet series, as a clue to the hidden complexity, which cannot be seen when the zeros are ostensibly fixed on the critical line and attempts are made to find abstract criteria which define those having only critical zeros aiming at an abstract proof of RH. We thus explore four examples, using richly different types



of tame and wild continuous transformation. These are much better viewed as movies from the link below, but here a series of stills with path diagrams will have to suffice.

They are all generated using a Mac software research application designed and developed by the author which is available at: <http://www.dhushara.com/DarkHeart/RZV/RZViewer.htm> and includes open source files for XCode compilation for flexible research use.

The first and tamest example is making a simple rotation between zeta and eta by using the multiplicative function connecting them:  $f(z, \theta) = (1 - (1 + e^{i\theta})2^{-z})$ ,  $\theta = 0, \dots, 2\pi$ . One can immediately see this will have periodic zeros at  $z = \ln(1 + e^{i\theta}) / \ln 2$  since

$1 - (1 + e^{i\theta})2^{-z} = 0 \Leftrightarrow (1 + e^{i\theta})2^{-z} = 1 \Leftrightarrow (1 + e^{i\theta}) = 2^z = e^{z \ln 2} \Leftrightarrow z \ln 2 = \ln(1 + e^{i\theta})$ , and that  $x \rightarrow -\infty$ , as  $\theta \rightarrow \pi$ , so that the periodic zeros on the line  $x = 1$  in eta will plunge into the negative real half-plane as we cross zeta. This is confirmed in fig 18, where we are able to use the functional equation throughout.

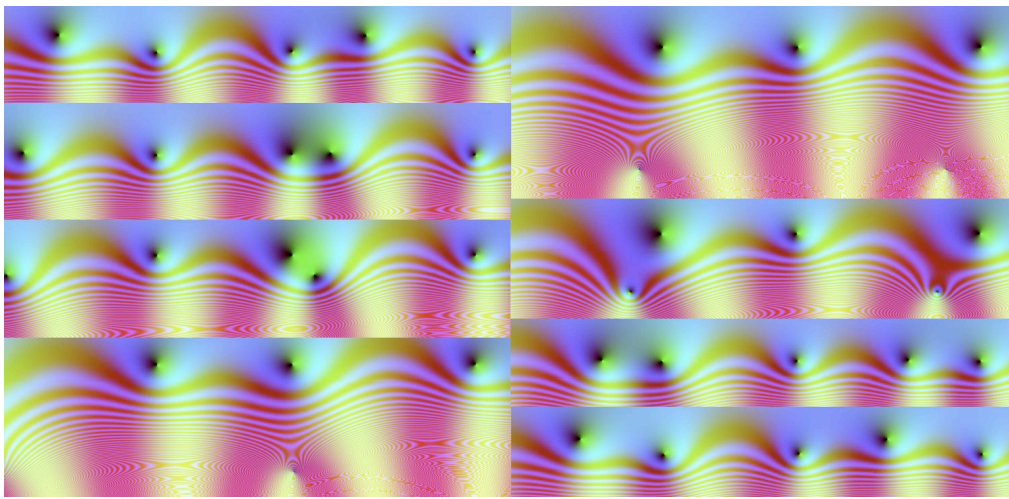
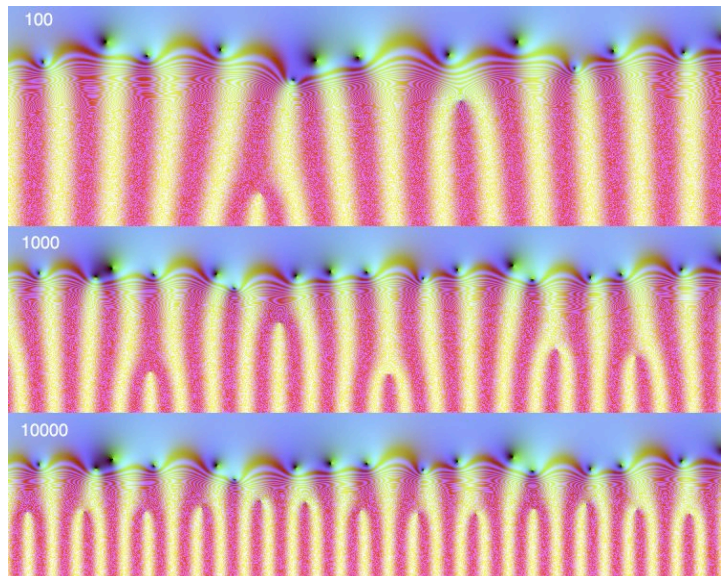


Fig 18: A continuous rotation from eta (top left) through zeta (between bottom left and top right) and back to eta (bottom right) shows the periodic zeros crossing the critical line and plunging asymptotically into the negative real half-plane as we cross zeta, subsequently being picked up by rising zeros spaced between the originals.

We now need to examine continuous transformations of functions that cannot be represented for negative real values using a functional equation, so we need to understand the consequences of using naked Dirichlet series functions in the forbidden zone. With one transitional exception in the last case, the examples are broadly confined to alternating series which are well-defined and convergent in the critical strip  $0 < x < 1$  however for  $x < 0$  these can become singular as the number of terms in the series increases in the limit to infinity. Fig 19 gives a portrait of a section of the function in fig 1 when the iterations are increased through two orders of magnitude, and as can be seen, there is increasing instability in the forbidden zone with increasing numbers of ‘gollum’ zeros closer and closer to  $x = 0$ .

Fig 19: The non- $L$ -function with  $\chi = \{0, 1, 0, -1, 0, 0, 1, 0, -1\}$  in the neighbourhood of  $\frac{1}{2} + 230i$  represented naked with 100, 1000 and 10000 series terms, shows increasingly extreme fluctuations in the forbidden zone with increasing numbers of ‘gollum’ zeros falling closer and closer to  $x = 0$ . However the approximation to the zeros in the critical strip  $0 < x < 1$  is sufficiently close by 1000 that little subsequent change is observable by including 10000 terms.





However, while the approximation is inaccurate for 100 terms at this imaginary range, by 1000 terms, increasing the terms to 10000 has little effect on the zeros in the critical strip, showing that a finite approximation suffices, as a numerical analytic tool, if the number of terms is over a suitable bound, which varies with the imaginary value of the neighbourhood being investigated.

For the next example, we explore a continuous transformation between  $L(6,2)$  with character cast  $\chi = \{0,1,0,0,0,-1\}$  and  $\chi = \{0,1,0,0,-1,0\}$ , which corresponds to the alternating Dirichlet series having the arithmetic progression  $\sum_{n=0}^{\infty} (-1)^n (1+3(n-1))^{-z}$ . The corresponding series for 2 is  $L(4,2)$  with character series  $\chi = \{0,1,0,-1\}$ , all of whose non-trivial zeros are on the critical line, but this is not the case for the above series, as shown in fig 5.

To make a continuous transformation requires moving off the natural numbers as bases. We will move continuously around a semicircular loop running firstly down the real axis from  $6n+5$  to  $6n+4$  and then anti-clockwise around  $6n + \frac{1}{2}(9 + e^{i\theta})$ ,  $\theta = \pi, \dots, 2\pi$ .

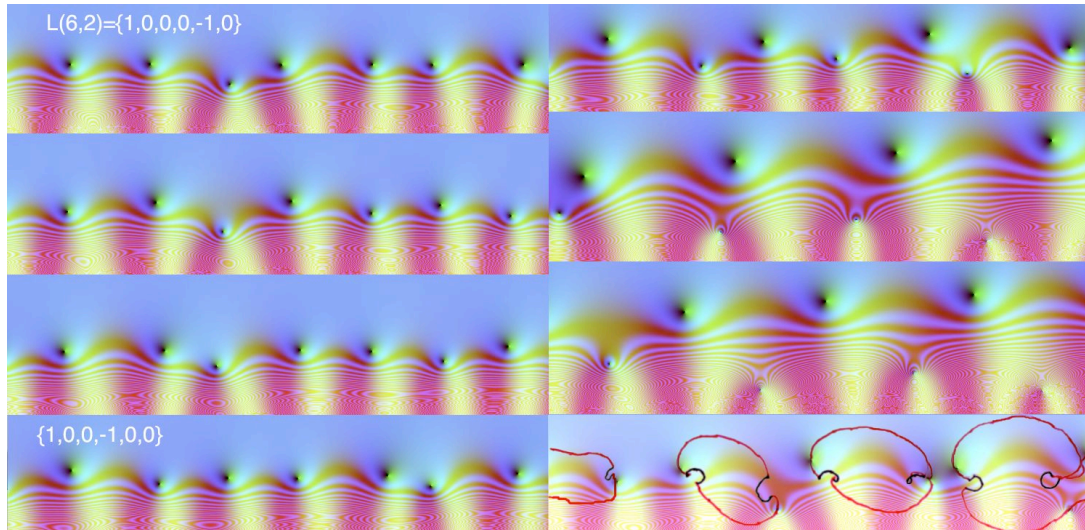


Fig 20: Continuous transformation between  $L(6,2)$  and the alternating arithmetic Dirichlet series with base  $(1+3(n-1))^{-z}$  left running down the real axis and right anti-clockwise around a semi-circle.

The bottom right image shows the orbits along the real line in black and round the semi-circle in red. The first part of the trajectory gives us a good idea of why the Riemann hypothesis might be true due to mode-locking, as the zeroes each follow local orbits approximating rotations, under the continuous transformation, so the zeros which are lined non-periodically on the critical line and periodically on  $x=0$  lose their phase relationships when we move from  $6n+5$  to  $6n+4$ , thus throwing the critical zeros ‘offline’.

However this neat picture is confounded by the dynamics we perceive on the semi-circular track, where pairs of zeros exchange places, plunging both deep into the ‘forbidden’ zone, and well up into the positive half-plane. Significantly the neat distinction between the critical non-periodic zeros and those on  $x=0$ , which satisfies the generalized Riemann hypothesis, that if a zero is in  $0 < x < 1$  then it is on  $x = \frac{1}{2}$ , is also lost, because critical and periodic zeros are interchanged. The dynamics of the zeros on the far left and right are not fully elucidated and may be periodic, or otherwise, as we shall see in following examples.

Note that the movement of the zeros is path-dependent and that continuous transformations can exchange the roles of critical, periodic forbidden ‘gollum’ zeros.

The next example takes this further into the wilderness, by examining changes in the character terms rather than the positions of the integer bases. We start with the character cast for  $L(10,4) = \{0,1,0,i,0,0,0,-i,0,-1\}$  and apply  $L(10,\theta) = \{0,1,0,e^{i\theta},0,0,0,-e^{i\theta},0,-1\}$ ,  $\theta=\pi/2,\dots,5\pi/2$ , a cyclic rotation, passing through  $L(10,2) = \{0,1,0,-i,0,0,0,i,0,-1\}$  at  $\theta = 3\pi/2$  and the non  $L$ -function  $\{0,1,0,-1,0,0,0,1,0,-1\}$ , at  $\theta=\pi$ .

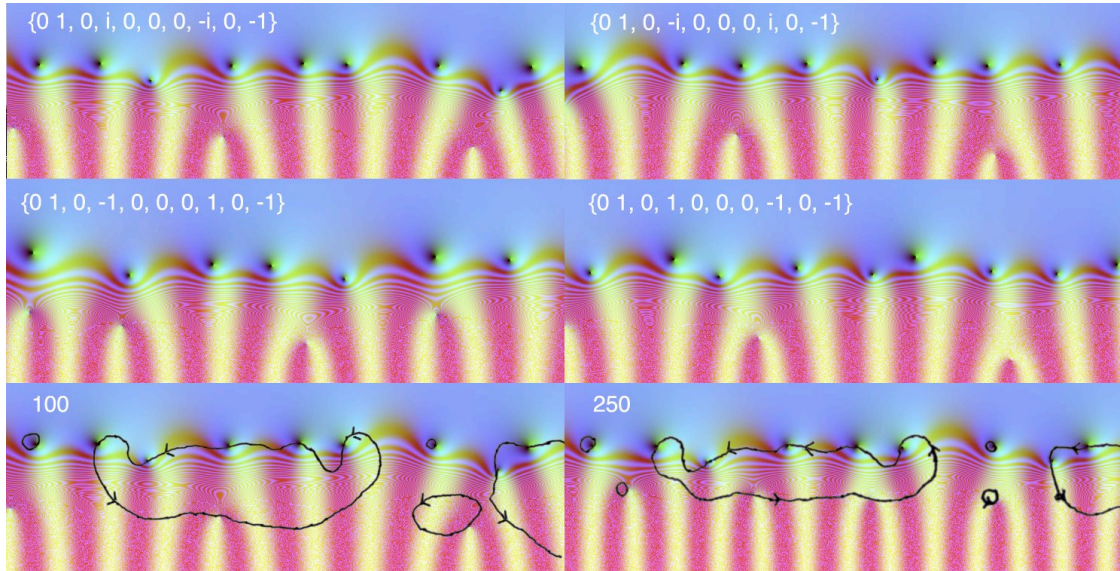


Fig 21: Cyclic rotation of the characters from  $L(10,4)$  to  $L(10,2)$  and back demonstrates ‘transmigration’ of the zeros, one step to the left each character cycle, in which critical, periodic and gollum zeros exchange positions. To assess the validity of approximation, using naked functions in the forbidden zone, the bottom two images compare the orbits for 100 and 250 iterations in a neighbourhood of  $\frac{1}{2}+24i$ . The central transmigration orbit is preserved and an additional gollum carrier zero has entered the loop.

As we move around the cycle, two of the critical zeros remain in small local closed orbits, but the rest, including both critical and periodic zeros, pass in a chain, from one to another, stepping once to the left for each complete cycle of rotation, exchanging places on the way with one of the ‘gollum’ zeros which should not exist in the negative real half-plane. In all it takes 10 cycles of the characters for a zero to move across the field of view.

This shows us that the dynamics of the critical zeros under continuous transformation of the function cannot be understood without taking into account the ‘gollum’ zeros in the naked representation that are eliminated in the functional equation representations of zeta and the  $L$ -functions, which have legitimate zeros only on  $y=0$ ,  $x=0$  and  $x=\frac{1}{2}$ .

To address the problem of the naked functions in the forbidden zone we took orbits for two different numbers of terms, 100 and 250, in a neighbourhood of  $\frac{1}{2}+24i$ . Intriguingly, although the increased number of terms has given rise to a greater number of gollums falling closer to the imaginary axis, the phase portrait of the orbits retains homology. The major transmigration cycle of the critical strip zeros is preserved by utilizing additional gollums as carriers. Other gollum and critical zeros have local closed orbits in both cases.

To take these examples to a fireworks finale, we have an example of another rotation of a character cast, this time of  $L(5,4)$  rotating each character by the factor implied by their position on the unit circle  $L(5,\theta) = \{0, e^{4i\theta}, e^{i\theta}, e^{3i\theta}, e^{2i\theta}\}$ ,  $\theta = \pi/2, \dots, 5\pi/2$ .



Fig 22: Character cast rotation of  $L(5,4)$  passes through three  $L$ -functions.

This is pushing the boundaries, because it is rotating the base of the constant term which could have been left static at 1, but it passes through three  $L$ -functions  $L(5,2) = \{0,1,-i,i,-1\}$  at  $3\pi/2$ ,  $L(5,3) = \{0,1,-1,-1,1\}$  at  $\pi$ , and  $L(5,4) = \{0,1,i,i,-1\}$  again at  $5\pi/2$ , and gives an excellent example of complex orbits in motion. A sine diagram of the rotations is shown in fig 22 with the three  $L$ -functions located.

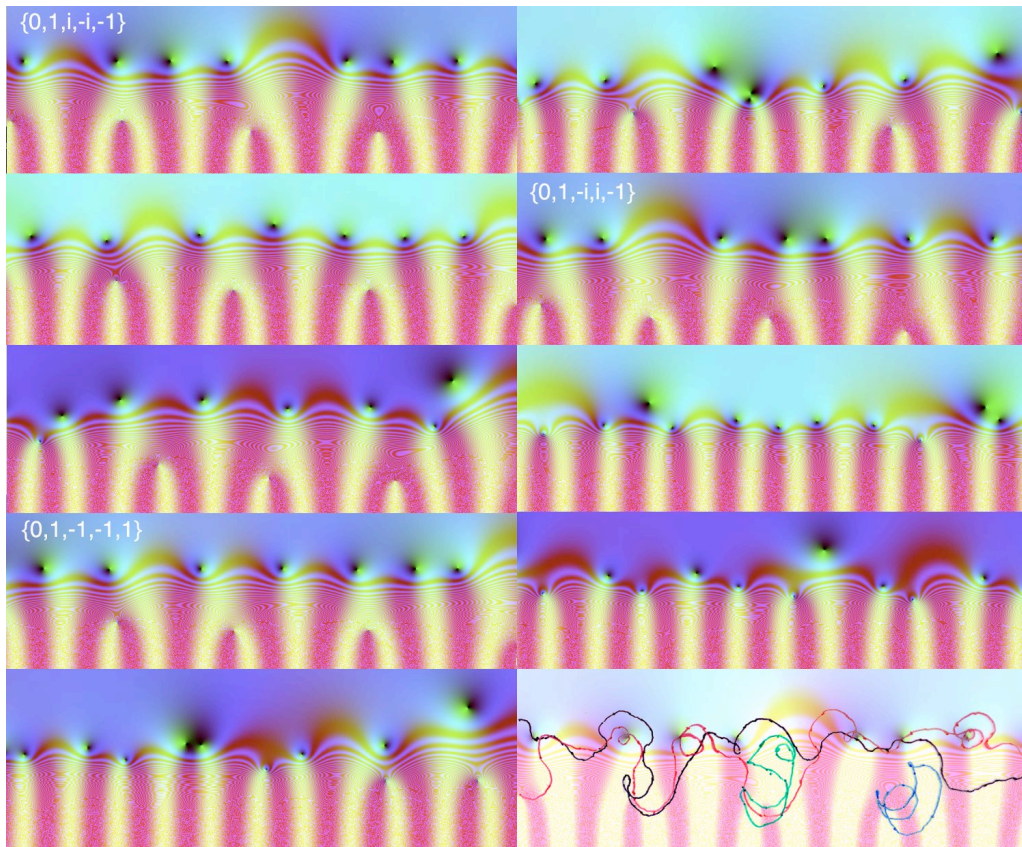
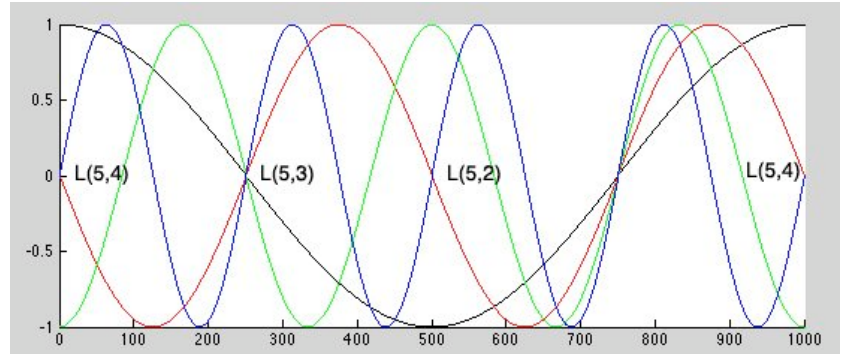


Fig 23: The character cast rotation of  $L(5,4)$  displaying complex entwined orbits again linking critical and 'gollum' zeros.

The orbits in this case have become very complex with many enclosed loops and 'entwined in the sense that successive zeros pass through almost identical paths before diverging again. As in the previous example the orbits involve critical zeros being carried into the position of 'gollum' zeros and vice versa as they pass along the same orbit.

In this case there are two migrating orbits shown in black and red in the bottom right illustration of the final state of  $L(5,4)$  carrying 4 and 3 critical zeros, with two of the 'gollum' zeros on complex closed orbits and one on the black migrating orbit. There are two near 'collisions', one very close to forming a degenerate zero in transition, top right.

## Conclusion

The Riemann hypothesis cannot be fully understood without decoding how the interference of the imaginary logarithmic wave functions results in the distribution of the zeros. Determining the orbits

of the zeros under continuous variation of the underlying functions provides a key. The confinement of the zeta and  $L$ -function zeros to the critical line appears to be caused by the primes being asymptotically as close to evenly distributed in relation to the logarithmic integral as they can possibly be, given that they cannot be evenly distributed and be prime. This suggests that the Riemann hypothesis is a consequence of minimal phase-locking in the imaginary wave functions, caused by the prime distribution, making convergence to zero possible in the asymptotic limit for  $\text{cis}(y \ln n)$  at the one 'index value' of  $n^{-1/2}$ , determining the power law trend in the absolute values of the terms. RH may thus be true, but unprovable, as a Turing halting problem, because the zeta, prime and Farey fraction definitions are logically equivalent, but no one can be proved to establish the truth of the others, thus giving all three a similar status to the axiom of choice as an additional postulate about asymptotic infinities.

## References

- Booker, A (2006) *Turing and the Riemann Hypothesis* Notices of the American Mathematical Society 53/10 1208-11.  
<http://www.ams.org/notices/200610/fea-booker.pdf>
- Booker, Andrew (2008) *Uncovering a New L-function* Notices of the American Mathematical Society 55/9 1088-94.  
<http://www.staff.science.uu.nl/~plaza101/Booker.pdf>
- Conrey, J. Brian (2003), *The Riemann Hypothesis* Notices of the American Mathematical Society 50/3 341-353,  
<http://www.ams.org/notices/200303/fea-conrey-web.pdf>.
- Daney Charles The Mathematics of Fermat's Last Theorem <http://cgd.best.vwh.net/home/flt/flt01.htm>
- Dokchitser, Tim <http://www.dpmms.cam.ac.uk/~td278/computel/> See also: <http://www.sagemath.org/>
- Franel, J.; Landau, E. (1924), *Les suites de Farey et le problème des nombres premiers*, Göttinger Nachr.: 198-206
- Garrett, Paul (2011) *Analytic continuation, functional equation: examples*  
[http://www.math.umn.edu/~garrett/m/mfms/notes\\_c/analytic\\_continuations.pdf](http://www.math.umn.edu/~garrett/m/mfms/notes_c/analytic_continuations.pdf)
- Hughes J. Shallit J., (1983) *On the Number of Multiplicative Partitions*, American Mathematical Monthly, 90(7) 468–471.
- Ingham, A.E. (1932, rep 1990), *The Distribution of Prime Numbers*, Cambridge University Press, MR1074573, ISBN 978-0-521-39789-6
- King C.C. Riemann Zeta Viewer <http://www.dhushara.com/DarkHeart/RZV/RZViewer.htm>
- Knopfmacher A, Mays M (2006) *Ordered and Unordered Factorizations of Integers* The Mathematica Journal 10:1 © Wolfram Media, Inc. <http://www.mathematica-journal.com/issue/v10i1/contents/Factorizations/Factorizations.pdf>
- Riemann, Bernhard (1859), *Über die Anzahl der Primzahlen unter einer gegebenen Grösse*, Monatsberichte der Berliner Akademie, <http://www.maths.tcd.ie/pub/HistMath/People/Riemann/Zeta/>.
- Weil, André (1948), *Sur les courbes algébriques et les variétés qui s'en déduisent*, Actualités Sci. Ind., no. 1041 = Publ. Inst. Math. Univ. Strasbourg 7 (1945), Hermann et Cie., Paris, MR0027151